

Fig. 3 continued

co-culture system is also considered to provide ATL cells with common factors with in vivo adhesion-dependent growth mechanism of ATL cells.

Although neoplastic cells of lymphoid malignancies have been considered to proliferate primarily in lymphoid tissues, there are so far few cell lines established from LN stroma and available for reproducible analysis of neoplastic cell growth. Since ATL cells frequently invade and proliferate in BM, especially in aggressive phase, this co-culture system is considered to provide components which are necessary for growth and survival of neoplastic cells in BM microenvironment. Surprisingly, we reported previously that in a semi-solid colony assay system, IL-2-dependent colony formation occurred in almost all cases of chronic or smoldering type, but rarely in acute and lymphoma types [55]. These results observed among our limited number of clinical cases indicate that in the prodromal phase of ATL, some cytokines were needed for the growth of neoplastic cells in vitro, while in a more aggressive phase, such a cytokine-dependency declines and some aberrant signal transducers might contribute to a more autonomous proliferation and enhance survival of ATL cells through anti-apoptotic process, which is considered to be closely related to stroma-dependent cell growth.

It has been demonstrated recently in several cancers, especially leukemias, that neoplastic cells are heterogeneous in terms of their capacity to grow and self renew, and that only a small proportion of cells are actually clonogenic in culture and also in vivo [56]. Many recent evidences indicate that microenvironment contributes significantly to tumorigenesis originated from such "cancer stem cells" [57]. In the present study, the leukemic CAFCs exhibited clonogenic potential by showing a linear relationship between inoculated ATL cells and CA numbers as carefully enumerated in the semi-solid collagen gel culture.

Furthermore, in four of eight acute-type cases, which gave rise to primary growth, we could observe the secondary CA formation in replating experiments (data not shown). Although it remains controversial whether there exists such a hierarchy in a malignant clone of ATL, our observation supports the hypothesis that there might be a neoplastic stem cell system also in ATL, and future studies on the cellular biology of leukemic CAFCs would shed light on our knowledge of this concept, especially in the context of interaction with the microenvironment of lymphohematopoietic tissue. This is important in that any treatment modality must eradicate such clonogenic cells that are quiescent or proliferating in close contact with stromal cells to obtain a cure.

In the present study, immunostaining and RNA-ISH analysis revealed that our co-culture system allowed the growth of primary ATL cells even with a trace amount of Tax, at the level of transcription and translation. On the other hand, expression of HBZ gene in ATL cells was not affected by our co-culture system. Interestingly, this difference in expression pattern of two genes apparently resembles the behavior of ATL cells in vivo. Together with the result of mRNA load assay in the adhesion blockade system and the finding of reappearance of Tax protein in ATL cell lines which grew upward from the CAs and detached from the MS-5 monolayer into the culture medium (data not shown), it is suggested that there might be a direct interaction between ATL cells and stromal layer as a regulatory mechanism of *tax* gene expression, including epigenetic modification, in this co-culture system. Furthermore, we believe that further investigation of the actions of the *HBZ* gene in this unique in vitro culture system is important to clarify not only regulatory mechanism of *tax* gene expression [58], but also interactions between microenvironment and ATL

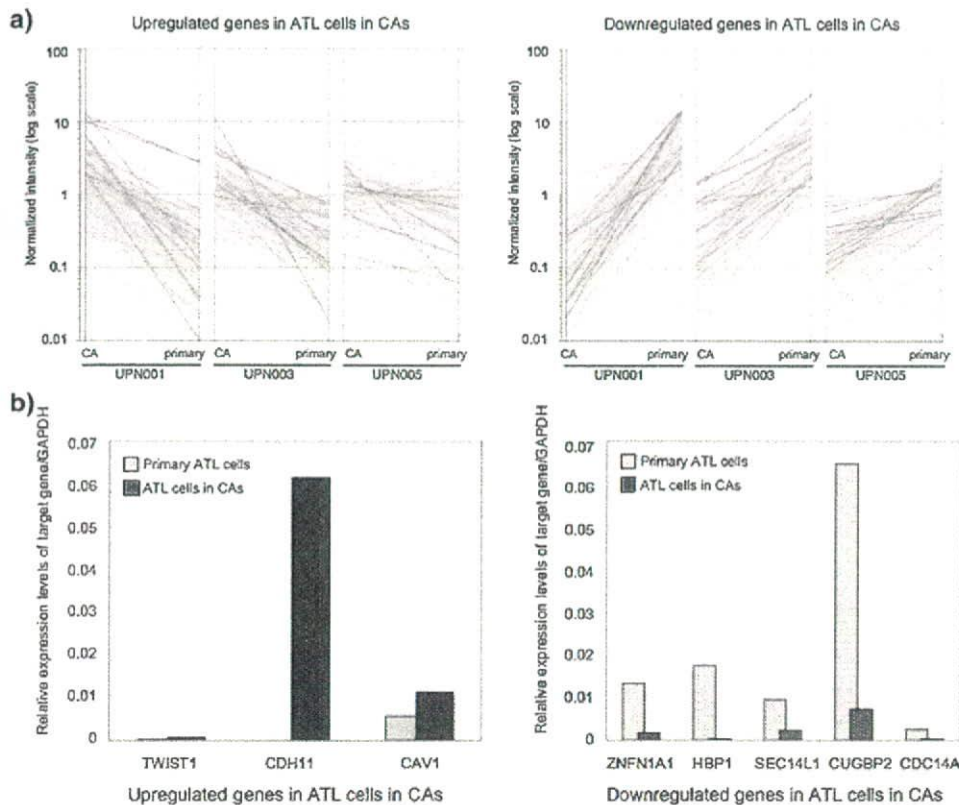


**Fig. 4** Comparative studies of gene expression profiles between ATL cells in CA and corresponding primary cells from three clinical samples. For the expression data set of subjects, we first set a condition in which the expression level of a given gene should receive the “Present” call [from Microarray Suite 5.0 (Affymetrix)] in at least 60% (four samples) of the samples, aiming to remove transcriptionally silent genes from the analysis. The mean expression intensity of the internal positive control probe sets ([http://www.affymetrix.com/support/technical/mask\\_files.affx](http://www.affymetrix.com/support/technical/mask_files.affx)) was set to 500U in each hybridization, and the fluorescence intensity of each test gene was normalized accordingly. **a** Diagrams of comparative profiles of three matched ATL cells in CA and their corresponding CD4<sup>+</sup> primary samples from the same individuals (UPN001, UPN003, and

UPN005); up-regulated genes (*left*) and down-regulated genes (*right*) in ATL cells in CA. **b** Validation of the expression of eight selected genes from the expression profiles by RTQ-PCR. Primers and probes used in this study are shown in Table 3. Results are expressed in *graphs* of primary cells (*light gray bars*) and those of ATL cells in CA (*dark gray bars*) as fold differences between samples in their target gene expression relative to their levels of GAPDH. Standard curves were generated for each gene with tenfold serial dilution ( $100 \times 10^{-6}$ ) of cDNA from the KOB cell line and lymphocytes obtained from healthy volunteers. After confirming the precise log-linear relation of the standard curve, the final results were expressed as fold differences between samples in their target gene expression relative to their levels of GAPDH

cells for their growth and survival. This co-culture system is considered to be useful for the analysis of ATL cell growth and survival in a condition without excessive effect of Tax which was always present in the former *in vitro* culture systems.

Application of transcriptional profiling of ATL cells in CA revealed that there were no significant difference between ATL cells composing CA and primary ATL cells in expression level of several molecules, which play important roles in signaling pathways in ATL, including NFkB pathway. NFkB and related molecules have been shown to be constitutively activated *in vivo* without expression of Tax [59], although the mechanism of the constitutive activation of NFkB is still unclear. Therefore, several essential signaling pathways could also contribute to the growth of ATL cells under the adhesion-dependent

and Tax-independent condition, which apparently resembles *in vivo* proliferation. On the other hand, interestingly also, we confirmed significant up- and down-regulation of several adhesion molecules and adaptor proteins, which play important roles in signaling pathways through cell-cell or cell-matrix interaction in ATL cells in CA. Taken together, these findings are assumed to indicate that our co-culture system might expose novel molecular mechanisms, which specifically regulate the growth and survival of clonogenic ATL cells. We believe that “outside-in” signaling pathways from interaction with the microenvironment might control such a mechanism in ATL cells. Further investigations are needed to elucidate the precise functions of these molecules.

Recently, a number of novel therapeutic agents to treat neoplastic diseases have been developed, as the growth



**Table 3** Genes whose expressions were up- or down-regulated in ATL cells in CA compared with corresponding primary cells as determined by microarray analysis and validated by RTQ-PCR

Gene title	Genbank Accession ID	Description	Primers	Product size	Fold change
Upregulated genes in CAs					
CDH11	D21254	Osteoblast-cadherin	S CTGGAACCATTTTTGTGATT AS TCCACCGAAAAATAGGGTTG	343 bp	32.93
TWIST1	X99268	Twist-related protein 1, H-Twist, Twist homolog 1 (acrocephalosyndactyly 3; Saethre-Chotzen syndrome)	S GTCCGCAGTCTTACGAGGAG AS CCAGCTTGAGGGTCTGAATC	159 bp	5.026
CAV1	AU147399	Caveolin 1, caveolae protein	S CGCACACCAAGGAGATCGA AS GTGTCCCTTCTGGTTCTGCAAT	106 bp	5.301
Downregulated genes in CAs					
CDC14A	NM_003672	CDC14 cell division cycle 14 homolog A	S GCACTTACAATCTCACCATTC AS CATGTTGTAATCCCTTTCTG	58 bp	0.0748
CUGBP2	N36839	CUG triplet repeat, RNA binding protein 2	S CCTTTGAGGACTGCCATTGT AS TGAGGGGGAAAGTCCTTTTT	236 bp	0.0723
SEC14L1	AI017770	SEC14 like 1 protein	S TCCAAGAGGTCCGACCAACCAC AS AGAGACCTGCAGGGACGCAA	288 bp	0.0686
HBP1	AI689935	High mobility group (HMG) box transcription factor 1	S GCTTCCTTTGCAATGGTTCT AS CTGTGCAGCTCACATCTGTATG	243 bp	0.0646
ZNFN1A1	NM_018563	DNA-binding protein Ikaros, Zinc finger protein, subfamily 1A, 1	S CGAGTTCTCGTCGCACATAA AS ATCAAACCCCAATCAACCAA	221 bp	0.0571

Matching primers and fluorescence probes were designed for each of the genes selected by microarray data, employing PRIMER3 software ([http://www.genome.wi.mit.edu/cgi-bin/primer/primer3\\_www.cgi](http://www.genome.wi.mit.edu/cgi-bin/primer/primer3_www.cgi)) using sequence data from the NCBI database

mechanism of neoplastic cells becomes clearer at the molecular level. We have previously reported that this co-culture system could be used to test the sensitivity of neoplastic progenitors of Philadelphia chromosome (Ph<sup>1</sup>)/BCR-ABL-positive leukemia to p210 tyrosine kinase inhibitor, imatinib mesylate (Gleevec<sup>TM</sup>) [18]. This observation provides evidence that our co-culture system is extremely valuable for testing human tumor cells to grow using similar signaling pathways as in vivo. IL-2-dependent T cell lines established from a bulk liquid culture were usually clonally different from primary ATL cells [60], whereas our co-culture system exhibited growth of primary ATL cells which were identical clone to clinical samples as shown in SBH analysis, indicating the superiority of our method for the study of primary ATL cells as a surrogate assay system to predict response of neoplastic progenitors to therapeutic candidate drugs.

## 5 Conclusion

The present study showed that our newly established ATL cell/murine stroma cell co-culture system is highly efficient for the assay of primary ATL cell growth. Further investigation should focus on the elucidation of novel disease-

specific signaling pathways starting from adhesion molecules and extracellular matrix proteins in this co-culture system, which contribute to adhesion-dependent proliferation and survival of ATL cells with a resemblance of expression pattern of proviral genes to that of in vivo ATL cells. This achievement might also be useful in developing novel therapeutic agents targeting ATL progenitors.

**Acknowledgments** The present study was supported by grants-in-aid from the Ministry of Education, Science and Culture of Japan (12670992) and by the twenty-first Century Center of Excellence (COE) Program of Nagasaki University "International Consortium for Medical Care of Hibakusha and Radiation Life Science".

## References

1. Uchiyama T, Yodoi J, Sagawa K, Takatsuki K, Uchino H. Adult T cell leukemia: clinical and hematologic features of 16 cases. *Blood*. 1977;50:481-92.
2. Takatsuki K. Adult T-cell leukemia. *Intern Med*. 1995;34:947-52.
3. Yoshida M, Miyoshi I, Hinuma Y. Isolation and characterization of retrovirus from cell lines of human adult T-cell leukemia and its implication in the disease. *Proc Natl Acad Sci USA*. 1982;79:2031-5.
4. Yoshida M, Seiki M, Yamaguchi K, Takatsuki K. Monoclonal integration of human T-cell leukemia provirus in all primary tumors of adult T-cell leukemia suggests causative role of human



- T-cell leukemia virus in the disease. *Proc Natl Acad Sci USA*. 1984;81:2534–7.
5. Arisawa K, Soda M, Endo S, Kurokawa K, Katamine S, Shimokawa I, et al. Evaluation of adult T-cell leukemia/lymphoma incidence and its impact on non-Hodgkin lymphoma incidence in southwestern Japan. *Int J Cancer*. 2000;85:319–24.
  6. Yasunaga J, Matsuoka M. Leukaemogenic mechanism of human T-cell leukaemia virus type I. *Rev Med Virol*. 2007;17:301–11.
  7. Aboud M, Golde DW, Bersch N, Rosenblatt JD, Chen IS. A colony assay for in vitro transformation by human T cell leukemia virus type 1 and type 2. *Blood*. 1987;70:432–6.
  8. Uchiyama T, Hori T, Tsudo M, Wano Y, Umadome H, Tamori S, et al. Interleukin-2 receptor (Tac antigen) expressed on adult T cell leukemia cells. *J Clin Invest*. 1985;76:446–53.
  9. Lunardi-Iskandar Y, Gessain A, Lam VH, Gallo RC. Abnormal in vitro proliferation and differentiation of T-cell colony forming cells in patients with tropical spastic paraparesis/human T lymphocyte virus type 1 (HTLV-1) associated myeloencephalopathy and healthy HTLV-1 carrier. *J Exp Med*. 1993;177:741–50.
  10. Seiki M, Hattori S, Hirayama Y, Yoshida M. Human adult T-cell leukemia virus: complete nucleotide sequence of provirus genome integrated in leukemia cell DNA. *Proc Natl Acad Sci USA*. 1983;80:3618–22.
  11. Yoshida M. Multiple viral strategies of HTLV-1 for dysregulation of cell growth control. *Annu Rev Immunol*. 2001;19:475–96.
  12. Basbous J, Gaudray G, Devaux C, Mesnard JM. Role of the human T-cell leukemia virus type I Tax protein in cell proliferation. *Recent Res Dev Mol Cell Biol*. 2002;3:155–66.
  13. Peloponese JM Jr, Kinjo T, Jeang KT. Human T-cell leukemia virus type 1 Tax and cellular transformation. *Int J Hematol*. 2007;86:101–6.
  14. Kinoshita T, Shimoyama M, Tobinai K, Ito M, Ito S, Ikeda S, et al. Detection of mRNA for the tax1/rex1 gene of human T-cell leukemia virus type-1 in fresh peripheral blood mononuclear cells of adult T-cell leukemia patients and viral carriers by using the polymerase chain reaction. *Proc Natl Acad Sci USA*. 1989; 86:5620–4.
  15. Ohshima K, Hashimoto K, Izumo S, Suzumiya J, Kikuchi M. Detection of human T lymphotropic virus type 1 (HTLV-1) DNA and mRNA in individual cells by polymerase chain reaction (PCR) in situ hybridization (ISH) and reverse transcription (RT)-PCR ISH. *Hematol Oncol*. 1996;14:91–100.
  16. Joh T, Yamada Y, Seto M, Kamihira S, Tomonaga M. High establishment efficiency of lymph node stromal cells which spontaneously produce multiple cytokines derived from adult T-cell leukemia/lymphoma patients. *Int J Oncol*. 1996;9:619–24.
  17. Itoh K, Tezuka H, Sakoda H, Konno M, Nagata K, Uchiyama T, et al. Reproducible establishment of hemopoietic supportive stromal cell lines from murine bone marrow. *Exp Hematol*. 1989;17:145–53.
  18. Kawaguchi Y, Jinnai I, Nagai K, Yagasaki F, Yakata Y, Matsuo T, et al. Effect of a selective Abl tyrosine kinase inhibitor, STI571, on in vitro growth of BCR-ABL-positive acute lymphoblastic leukemia cells. *Leukemia*. 2001;15:590–4.
  19. Maeda T, Yamada Y, Moriuchi R, Sugahara K, Tsuruda K, Joh T, et al. Fas gene mutation in the progression of adult T cell leukemia. *J Exp Med*. 1999;189:1063–71.
  20. Shimoyama M, Members of the Lymphoma Study Group. Diagnostic criteria and classification of clinical subtypes of adult T-cell leukemia-lymphoma. A report from the Lymphoma Study Group. *Br J Haematol* (1984–1987) 1991;79:428–37.
  21. Tanaka Y, Masuda M, Yoshida A, Shida H, Nyunoya H, Shimotohno K, et al. An antigenic structure of the trans-activator protein encoded by human T-cell leukemia virus type-1 (HTLV-1), as defined by a panel of monoclonal antibodies. *AIDS Res Hum Retroviruses*. 1992;8:227–35.
  22. Tanaka Y, Lee B, Inoi T, Tozawa H, Yamamoto N, Hinuma Y. Antigens related to three core proteins of HTLV-1 (p24, p19 and p15) and their intracellular localizations, as defined by monoclonal antibodies. *Int J Cancer*. 1986;37:35–42.
  23. Tsuji T, Ogasawara H, Aoki Y, Tsurumaki Y, Kodama H. Characterization of murine stromal cell clones established from bone marrow and spleen. *Leukemia*. 1996;10:803–12.
  24. Nagai K, Sohda H, Kuriyama K, Kamihira S, Tomonaga M. Usefulness of immunocytochemistry for phenotypical analysis of acute leukemia; improved fixation procedure and comparative study with flow cytometry. *Leuk Lymphoma*. 1995;16:319–27.
  25. Adams JC. Heavy metal intensification of DAB-based HRP reaction products. *J Histochem Cytochem*. 1981;29:775.
  26. Tsukasaki K, Ikeda S, Murata K, Maeda T, Atogami S, Sohda H, et al. Characteristics of chemotherapy-induced clinical remission in long survivors with aggressive adult T-cell leukemia/lymphoma. *Leuk Res*. 1993;17:157–66.
  27. Kamihira S, Dateki N, Sugahara K, Hayashi T, Harasawa H, Minami S, et al. Significance of HTLV-1 proviral load quantification by real-time PCR as a surrogate marker for HTLV-1-infected cell count. *Clin Lab Haematol*. 2003;25:111–7.
  28. Miyazato A, Kawakami K, Iwakura Y, Saito A. Chemokine synthesis and cellular inflammatory changes in lung of mice bearing p40tax of human T-lymphotropic virus type I. *Clin Exp Immunol*. 2000;120:113–24.
  29. Choi YL, Tsukasaki K, O'Neill MC, Yamada Y, Onimaru Y, Matsumoto K, et al. A genomic analysis of adult T-cell leukemia. *Oncogene*. 2007;26:1245–55.
  30. Usui T, Yanagihara K, Tsukasaki K, Murata K, Hasegawa H, Yamada Y, et al. Characteristic expression of HTLV-1 basic zipper factor (HBZ) transcripts in HTLV-1 provirus-positive cells. *Retrovirology*. 2008;5:34–44.
  31. Breems DA, Blokland EA, Neben S, Ploemacher RE. Frequency analysis of human primitive hematopoietic stem cell subsets using a cobblestone area forming cell assay. *Leukemia*. 1994;8:1095–104.
  32. Satou Y, Yasunaga J, Yoshida M, Matsuoka M. HTLV-I basic leucine zipper factor gene mRNA supports proliferation of adult T cell leukemia cells. *Proc Natl Acad Sci USA*. 2006;103:720–5.
  33. Mesnard JM, Barbeau B, Devaux C. HBZ, a new important player in the mystery of adult T-cell leukemia. *Blood*. 2006;108:3979–82.
  34. Tomita K, van Bokhoven A, van Leenders GJ, Ruijter ET, Jansen CF, Bussemakers MJ, et al. Cadherin switching in human prostate cancer progression. *Cancer Res*. 2000;60:3650–4.
  35. Alexander NR, Tran NL, Rekapally H, Summers CE, Glackin C, Heimark RL. *N-cadherin* Gene Expression in Prostate Carcinoma Is Modulated by Integrin-Dependent Nuclear Translocation of Twist1. *Cancer Res*. 2006;66:3365–9.
  36. Williams TM, Lisanti MP. Caveolin-1 in oncogenic transformation, cancer, and metastasis. *Am J Physiol Cell Physiol*. 2005;288:494–506.
  37. Paulsen MT, Starks AM, Derheimer FA, Hanasoge S, Li L, Dixon JE, et al. The p53-targeting human phosphatase hCdc14A interacts with the Cdk1/cyclin B complex and is differentially expressed in human cancers. *Mol Cancer*. 2006;5:25.
  38. Mukhopadhyay D, Houchen CW, Kennedy S, Dieckgraefe BK, Anant S. Coupled mRNA Stabilization and Translational Silencing of Cyclooxygenase-2 by a Novel RNA Binding Protein, CUGBP2. *Mol Cell*. 2003;11:113–26.
  39. Zhang X, Kim J, Ruthazer R, McDevitt MA, Wazer DE, Paulson KE, et al. The HBPI transcriptional repressor participates in RAS-induced premature senescence. *Mol Cellular Biol*. 2006; 26:8252–66.



40. Rebollo A, Schmitt C. Ikaros, Aiolos and Helios: transcription regulators and lymphoid malignancies. *Immunol Cell Biol.* 2003;81:171–5.
41. Issaad C, Croisille L, Katz A, Vainchenker W, Coulombel M. A murine stromal cell line allows the proliferation of very primitive human CD34<sup>+</sup>/CD38<sup>-</sup> progenitor cells in long-term cultures and semisolid assays. *Blood.* 1993;81:2916–24.
42. Bajénoff M, Egen JG, Koo LY, Laugier JP, Brau F, Glaichenhaus N, et al. Stromal cell networks regulate lymphocyte entry, migration, and territoriality in lymph nodes. *Immunity.* 2006;25:989–1001.
43. Woolf E, Grigorova I, Sagiv A, Grabovsky V, Feigelson SW, Shulman Z, et al. Lymph node chemokines promote sustained T lymphocyte motility without triggering stable integrin adhesiveness in the absence of shear forces. *Nat Immunol.* 2007;8:1076–85.
44. Mitsiades CS, McMillin DW, Klippel S, Hideshima T, Chauhan D, Richardson PG, et al. The role of the bone marrow microenvironment in the pathophysiology of myeloma and its significance in the development of more effective therapies. *Hematol Oncol Clin North Am.* 2007;21:1007–34.
45. Lwin T, Hazlehurst LA, Dessureault S, Lai R, Bai W, Sotomayor E, et al. Cell adhesion induces p27Kip1-associated cell-cycle arrest through down-regulation of the SCFSkp2 ubiquitin ligase pathway in mantle-cell and other non-Hodgkin B-cell lymphomas. *Blood.* 2007;110:1631–8.
46. Tanaka Y, Kimata K, Wake A, Mine S, Morimoto I, Yamakawa N, et al. Heparan sulfate proteoglycan on leukemic cells is primarily involved in integrin triggering and its mediated adhesion to endothelial cells. *J Exp Med.* 1996;184:1987–97.
47. Imura A, Hori T, Imada K, Kawamata S, Tanaka Y, Imamura S, et al. OX40 expressed on fresh leukemic cells from adult T-cell leukemia patients mediates cell adhesion to vascular endothelial cells: implications for the possible involvement of OX40 in leukemic cell infiltration. *Blood.* 1997;89:2951–8.
48. Hiraiwa N, Hiraiwa M, Kannagi R. Human T-cell leukemia virus-1 encoded Tax protein transactivates alpha 1 → 3 fucosyltransferase Fuc-T VII, which synthesizes sialyl Lewis X, a selectin ligand expressed on adult T-cell leukemia cells. *Biochem Biophys Res Commun.* 1997;231:183–6.
49. Tanaka Y, Minami Y, Mine S, Hirano H, Hu CD, Fujimoto H, et al. H-Ras signals to cytoskeletal machinery in induction of integrin-mediated adhesion of T cells. *J Immunol.* 1999;163:6209–16.
50. Sasaki H, Nishikata I, Shiraga T, Akamatsu E, Fukami T, Hidaka T, et al. Overexpression of a cell adhesion molecule, TSLC1, as a possible molecular marker for acute-type adult T-cell leukemia. *Blood.* 2005;105:1204–13.
51. Suzuki J, Fujita J, Taniguchi S, Sugimoto K, Mori KJ. Characterization of murine hematopoietic-supportive (MS-1 and MS-5) and non-supportive (MS-K) cell lines. *Leukemia.* 1992;6:452–8.
52. Tsuji T, Waga I, Tezuka K, Kamada M, Yatsunami K, Kodama H. Integrin beta2 (CD18)-mediated cell proliferation of HEL cells on a hematopoietic-supportive bone marrow stromal cell line, HESS-5 cells. *Blood.* 1998;91:1263–71.
53. Dewan MZ, Terashima K, Taruishi M, Hasegawa H, Ito M, Tanaka Y, et al. Rapid tumor formation of human T-cell leukemia virus type 1-infected cell lines in novel NOD-SCID/gamma-mac(null) mice: suppression by an inhibitor against NF-kappaB. *J Virol.* 2003;77:5286–94.
54. Imada K, Takaori-Kondo A, Akagi T, Shimotohno K, Sugamura K, Hattori T, et al. Tumorigenicity of human T-cell leukemia virus type 1-infected cell lines in severe combined immunodeficient mice and characterization of the cells proliferating in vivo. *Blood.* 1995;86:2350–7.
55. Hata T, Fujimoto T, Tsushima H, Murata K, Tsukasaki K, Atogami S, et al. Multi-clonal expansion of unique human T-lymphotropic virus type-1-infected T cells with high growth potential in response to interleukin-2 in prodromal phase of adult T cell leukemia. *Leukemia.* 1999;13:215–21.
56. Reya T, Morrison SJ, Clarke MF, Weissman IL. Stem cells, cancer, and cancer stem cells. *Nature.* 2001;414:105–11.
57. Bissell MJ, LaBarge MA. Context, tissue plasticity, and cancer: Are tumor stem cells also regulated by the microenvironment? *Cancer Cell.* 2005;7:17–23.
58. Gaudray G, Gachon F, Basbous J, Biard-Piechaczyk M, Devaux C, Mesnard JM. The complementary strand of the human T-cell leukemia virus type 1 RNA genome encodes a bZIP transcription factor that down-regulates viral transcription. *J Virol.* 2002;76:12813–22.
59. Mori N, Fujii M, Ikeda S, Yamada Y, Tomonaga M, Ballard DW, et al. Constitutive activation of NF-kappaB in primary adult T-cell leukemia cells. *Blood.* 1999;93:2360–8.
60. Yamada Y, Nagata Y, Kamihira S, Tagawa M, Ichimaru M, Tomonaga M, et al. IL-2-dependent ATL cell lines with phenotypes differing from the original leukemia cells. *Leukemia Res.* 1991;15:619–25.



ORIGINAL ARTICLE

# The FLT3 inhibitor PKC412 exerts differential cell cycle effects on leukemic cells depending on the presence of FLT3 mutations

T Odgerel<sup>1</sup>, J Kikuchi<sup>1</sup>, T Wada<sup>1</sup>, R Shimizu<sup>1</sup>, K Futaki<sup>1</sup>, Y Kano<sup>2</sup> and Y Furukawa<sup>1</sup>

<sup>1</sup>Division of Stem Cell Regulation, Center for Molecular Medicine, Jichi Medical School, Tochigi, Japan and <sup>2</sup>Division of Hematology, Tochigi Cancer Center, Tochigi, Japan

**PKC412 is a staurosporine derivative that inhibits several protein kinases including FLT3, and is highly anticipated as a novel therapeutic agent for acute myeloblastic leukemia (AML) carrying FLT3 mutations. In this study, we show that PKC412 exerts differential cell cycle effects on AML cells depending on the presence of FLT3 mutations. PKC412 elicits massive apoptosis without markedly affecting cell cycle patterns in AML cell lines with FLT3 mutations (MV4-11 and MOLM13), whereas it induces G<sub>2</sub> arrest but not apoptosis in AML cell lines without FLT3 mutations (THP-1 and U937). In MV4-11 and MOLM13 cells, PKC412 inactivates Myt-1 and activates CDC25c, leading to the activation of CDC2. Activated CDC2 phosphorylates Bad at serine-128 and facilitates its translocation to the mitochondria, where Bad triggers apoptosis. In contrast, PKC412 inactivates CDC2 by inducing serine-216 phosphorylation and subsequent cytoplasmic sequestration of CDC25c in THP-1 and U937 cells. As a result, cells are arrested in the G<sub>2</sub> phase of the cell cycle, but do not undergo apoptosis because Bad is not activated. The FLT3 mutation-dependent differential cell cycle effect of PKC412 is considered an important factor when PKC412 is combined with cell cycle-specific anticancer drugs in the treatment of cancer and leukemia.**

*Oncogene* (2008) 27, 3102–3110; doi:10.1038/sj.onc.1210980; published online 10 December 2007

**Keywords:** FLT3 inhibitor; leukemia; cell cycle; CDC2; CDC25; Bad

## Introduction

FMS-like tyrosine kinase-3 (FLT3) is a member of class III receptor tyrosine kinases, and is expressed on hematopoietic stem/progenitor cells. The binding of FLT3 ligand induces dimerization and autophosphoryla-

tion of FLT3, and subsequently activates multiple signal transduction pathways favoring cell survival and proliferation (Lyman *et al.*, 1993; Small *et al.*, 1994). FLT3 is also expressed in the majority of acute leukemias and is overexpressed in many cases (Gilliland and Griffin, 2002). In addition, its mutations are found in approximately 30% of patients with acute myeloblastic leukemia (AML), and accordingly, these are the second most common genetic alterations in AML. FLT3 mutations include internal tandem duplication of the juxtamembrane domain (FLT3-ITD) and point mutations in the activating loop, both of which result in ligand-independent activation of FLT3. The constitutive activation of FLT3 appears to promote aberrant proliferation and survival of hematopoietic stem/progenitor cells, leading to leukemogenesis (Kelly *et al.*, 2002).

Because of the high frequency of mutations and overexpression, FLT3 should be an appropriate therapeutic target in AML (Griffin, 2004). It has been shown that the staurosporine derivative PKC412 inhibits multi-target tyrosine kinases, including FLT3, protein kinase C, CDC2 and receptors for PDGF, FGF and VEGF (Levis and Small, 2005). PKC412 induces apoptosis in blasts from AML patients with FLT3 mutations, and prolongs survival in animal models of FLT3-induced myeloproliferative diseases (Weisberg *et al.*, 2002). Clinical trials for patients with solid tumors and AML revealed that PKC412 alone yielded limited clinical activity (Propper *et al.*, 2001; Stone *et al.*, 2005). To overcome this limitation, it is reasonable to combine PKC412 with other conventional antileukemic agents.

Recently, we have reported that PKC412 has synergistic effects with most antileukemic agents for FLT3-mutated leukemia cell lines (Furukawa *et al.*, 2007). In contrast, PKC412 is antagonistic to most drugs, except for those inducing mitotic arrest or active in the G<sub>2</sub>/M phase in leukemia cell lines without FLT3 mutations. This finding provides useful information for the design of effective combination therapy containing PKC412. For safe and effective clinical applications, however, it is essential to clarify the molecular basis of the FLT3 mutation-dependent divergence of leukemic cell responses to PKC412. In this study, we attempted to resolve this issue by analysing the effects of PKC412 on the expression of cell cycle regulators and Bcl-2 family proteins in AML cell lines with or without FLT3 mutations.

Correspondence: Professor Y Furukawa, Division of Stem Cell Regulation, Center for Molecular Medicine, Jichi Medical School, 3311-1 Yakushiji, Shimotsuke, Tochigi 329-0498, Japan.  
 E-mail: furuyu@jichi.ac.jp

Received 2 July 2007; revised 5 November 2007; accepted 6 November 2007; published online 10 December 2007



**Results**

*Effects of PKC412 on growth kinetics of AML cell lines with or without FLT3 mutations*

We first compared the sensitivity to PKC412 of four AML cell lines: MOLM13, MV4-11, THP-1 and U937. It has been shown that MOLM13 and MV4-11 cell lines carry FLT3-ITD (internal tandem duplication), whereas FLT3 is in wild-type configuration in THP-1 and U937 cell lines (Quentmeier *et al.*, 2003). THP-1 cells express a large amount of FLT3 but U937 cells do not express FLT3 (Yao *et al.*, 2003). In pilot experiments, we determined the dose–response curves at day 3 (data not shown), and calculated the IC<sub>50</sub> values for MOLM13, MV4-11, THP-1 and U937 to be 38 ± 4, 34 ± 6, 116 ± 26 and 207 ± 41 nM, respectively. On the basis of this result, we treated these cell lines with 100 nM PKC412 and observed the changes in growth kinetics. As shown in Figure 1a, PKC412 almost completely inhibited an increase in cell numbers of MOLM13 and MV4-11 cell lines. Growth inhibition was accompanied by the abrogation of constitutive phosphorylation of FLT3 (Figure 1b). The effects of PKC412 on other possible targets were variable and not correlated with cytotoxicity (Figure 1c and Supplementary Figure 1), suggesting that FLT3 is a principal target of PKC412-mediated growth inhibition of MOLM13 and MV4-11 cells. The proliferation of THP-1 cells was also markedly suppressed by PKC412, whereas U937 cells were relatively resistant to the drug (Figure 1a, lower panel). It is of

note that the steady-state growth of AML cell lines with FLT3 mutations (MOLM13 and MV4-11) was significantly slower than that of AML cell lines without FLT3 mutations (THP-1 and U937) (Figure 1a, upper panel).

*Cell cycle analysis of PKC412-treated AML cell lines*

Next, we attempted to clarify the underlying mechanisms of PKC412-mediated growth inhibition of AML cell lines using cell cycle analysis. PKC412-induced apoptosis, as judged by an increase in the size of the sub-G<sub>1</sub> fraction (see Figure 2a for representative results, and Table 1 for quantification and statistical analysis of three independent experiments), DNA fragmentation (Figure 2b) and the appearance of apoptotic bodies (Figure 2c), in MOLM13 and MV4-11 cell lines after 24 h of culture without markedly affecting cell cycle distribution except for a minor decrease in the fraction of cells in the growth phases (S and G<sub>2</sub>/M phases). In contrast, THP-1 and U937 cells were arrested in the G<sub>2</sub> phase by PKC412 after 12 h of treatment, and underwent mitotic slippage to become hyperploid after 48 h, especially in the latter (Figure 2 and Table 1). Apoptosis was barely observed in these cell lines up to 48 h of culture.

The difference of the changes in cell cycle distribution between PKC412-treated AML cell lines with FLT3-ITD and those with wild-type FLT3 may provoke the differential responses of cells to the combination of PKC412 and cell cycle-modifying drugs. To verify this

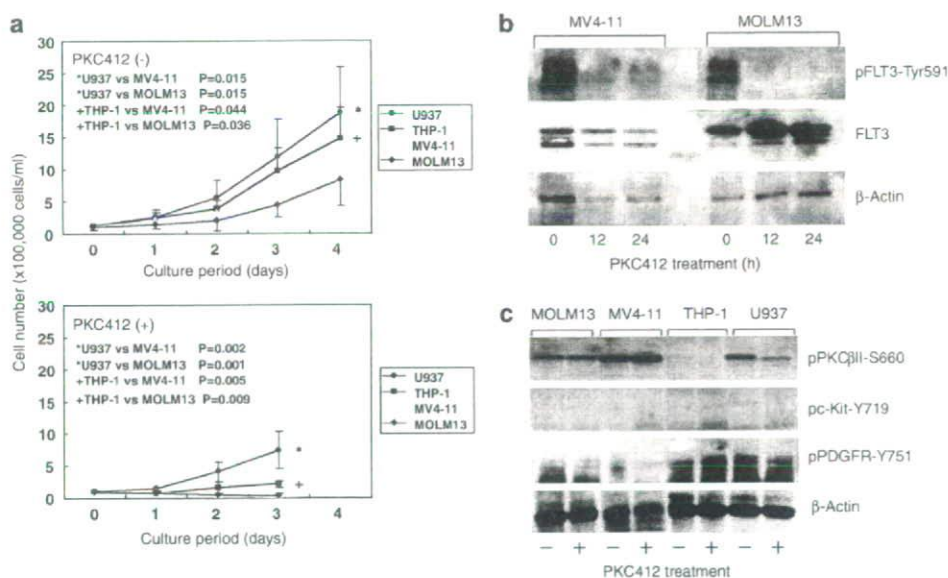


**Figure 1** Effects of PKC412 on cell growth and FLT3 phosphorylation of acute myeloblastic leukemia (AML) cell lines. (a) We seeded AML cell lines at an initial concentration of  $1 \times 10^5$  cells ml<sup>-1</sup>, and cultured in the absence (upper panel) or presence (lower panel) of 100 nM PKC412 for up to 4 days. Viable cells were counted after staining with erythrosine B dye. The means ± s.d. (bars) of three independent experiments are shown. Statistical analysis was performed using Student's *t*-test. (b) Whole cell lysates were prepared from MV4-11 and MOLM13 cells cultured with 100 nM PKC412 at the indicated time points, and subjected to immunoblotting with an antibody that specifically recognizes FLT3 phosphorylated at tyrosine-591 (pFLT3-Tyr591). The membranes were reblotted with anti-FLT3 and β-actin antibodies to serve as loading controls. (c) Whole cell lysates were prepared from four cell lines before (–) and after (+) culture with 100 nM PKC412 for 24 h, and used for the detection of the indicated proteins. Data shown are representative of multiple independent experiments.



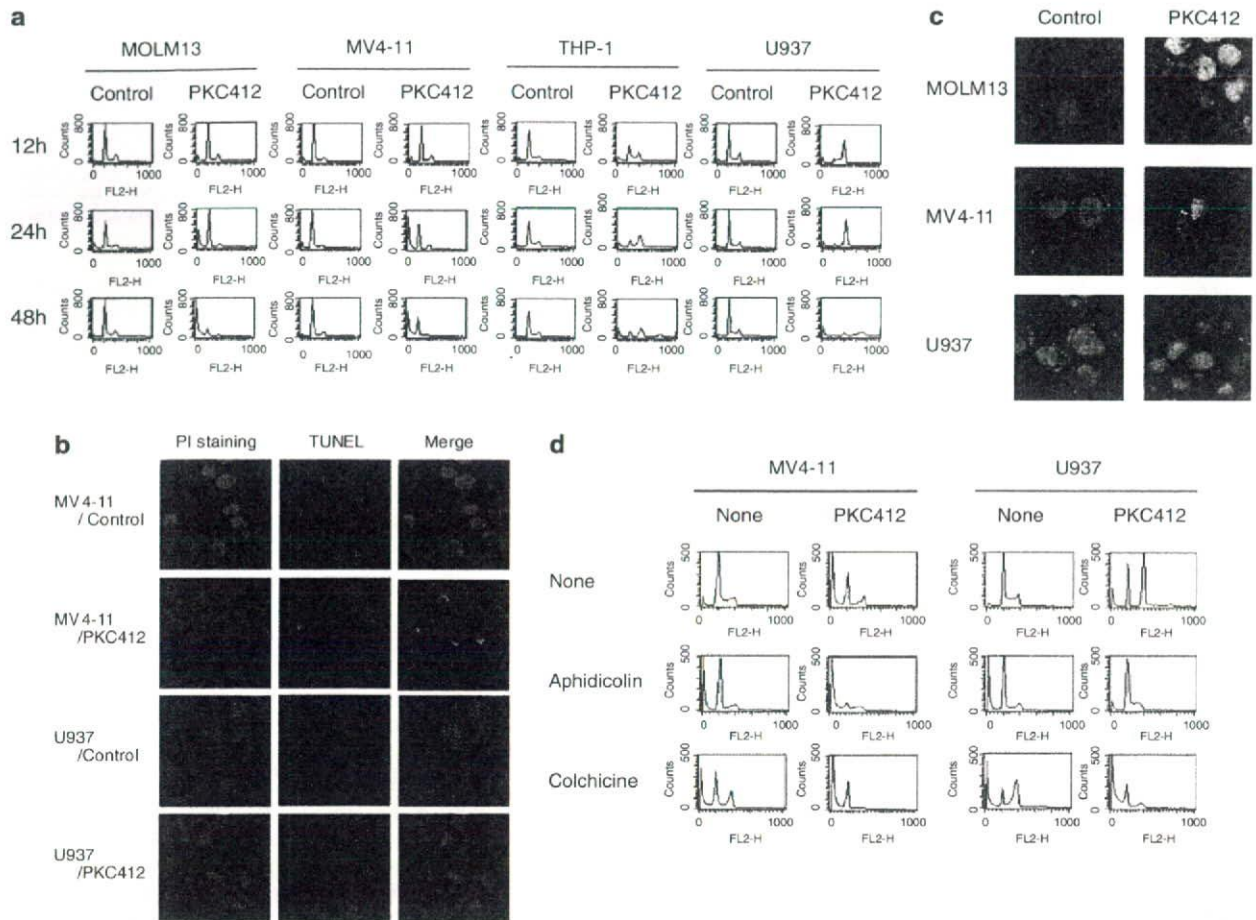


**Figure 2** Differential effects of PKC412 on the cell cycle of acute myeloblastic leukemia (AML) cell lines with or without FLT3 mutations. MOLM13, MV4-11, THP-1 and U937 cells were seeded at  $1 \times 10^5$  cells  $\text{ml}^{-1}$ , and cultured in the absence (control) or presence (PKC412) of 100 nM PKC412. **(a)** Cells were harvested at the indicated time points, and stained with propidium iodide in preparation for cell cycle analysis. See Table 1 for quantification and statistical analysis. **(b)** After 24 h of culture, cells were harvested for the detection of DNA fragmentation by the TUNEL method. Fragmented DNA was labeled with biotin-dUTP and stained with avidin-conjugated fluorescein isothiocyanate (FITC; TUNEL). Intact DNA was counterstained with propidium iodide (PI staining). Original magnification is  $\times 400$  for all panels. **(c)** After 24 h of culture, cells were stained with an antitubulin antibody (green fluorescence) and propidium iodide (red fluorescence). Original magnification is  $\times 600$  for all panels. **(d)** MV4-11 and U937 cells were cultured with (aphidicolin and colchicine) or without (none) cell cycle-modifying drugs in the absence (none) or presence (PKC412) of PKC412. The concentrations of each drug were PKC412 100 nM, aphidicolin 1  $\text{mg ml}^{-1}$  and colchicine 100 nM. After 24 h of culture, cells were harvested for cell cycle analysis. The data shown are representative of three independent experiments.

hypothesis, we examined the combined effects of PKC412 and either aphidicolin, which induces  $G_1/S$  arrest by inhibiting DNA polymerase  $\alpha$ , or colchicine, which arrests cells at mitosis by disrupting mitotic spindle. As shown in Figure 2d, PKC412 was synergistic with both aphidicolin and colchicine in MV4-11 cells, but only with colchicine in U937 cells. This is fully consistent with the pattern of cell cycle changes induced by PKC412 in each cell line.

#### *PKC412 differentially modulates the phosphorylation of CDC2 in AML cell lines depending on the presence of FLT3 mutations*

The above results indicate that PKC412 inhibits the growth of AML cells via distinct mechanisms depending on the presence of FLT3 mutations. We investigated the

underlying mechanisms of differential responses to PKC412. First, we checked the phosphorylation status of CDC2, which reflects its activity *in vivo*, in PKC412-treated AML cell lines. As shown in Figure 3a, CDC2 was heavily phosphorylated at tyrosine-15, an ATP-binding site critical for the kinase function of CDC2 (Watanabe *et al.*, 1995), in untreated MOLM13 and MV4-11 cells. In contrast, CDC2-tyrosine 15 phosphorylation was not prominent in untreated THP-1 and U937 cells. These results suggest that CDC2 is relatively inactive in AML cell lines with FLT3 mutations, but is constitutively active in AML cell lines with wild-type FLT3. This pattern is fully compatible with the steady-state growth kinetics of these cells (Figure 1a). PKC412 modified the phosphorylation state of CDC2 in a reciprocal manner dependent on the presence of FLT3 mutations: CDC2 phosphorylation decreased



**Table 1** Effects of PKC412 on cell cycle distribution of acute myeloblastic leukemia (AML) cell lines\*

	MOLM13			MV4-11			THP-1			U937		
	Control	PKC412	P-value*	Control	PKC412	P-value*	Control	PKC412	P-value*	Control	PKC412	P-value*
<i>12 h</i>												
Sub-G <sub>1</sub>	4.6±0.9	9.7±3.2	<b>0.04880</b>	5.6±0.8	6.8±1.7	0.21342	3.7±0.7	6.3±1.0	0.06957	3.7±0.8	3.3±0.8	0.21961
G <sub>1</sub>	79.1±1.4	73.7±5.4	0.15931	82.6±3.2	81.2±1.8	0.36663	71.7±6.3	61.2±2.0	0.10660	79.3±2.2	22.1±3.4	<b>0.00022</b>
S+G <sub>2</sub> /M	16.3±0.9	16.6±3.0	0.46585	11.8±2.5	12.0±2.7	0.47673	24.5±5.7	32.5±1.9	0.13740	17.1±2.6	74.6±4.2	<b>0.00023</b>
<i>24 h</i>												
Sub-G <sub>1</sub>	7.8±0.7	14.4±2.9	<b>0.02911</b>	6.8±1.6	31.3±3.3	<b>0.00974</b>	2.6±0.7	3.8±0.7	0.13211	3.7±1.0	3.2±0.8	0.35510
G <sub>1</sub>	72.0±1.8	79.2±2.8	<b>0.00553</b>	82.0±0.6	56.7±3.8	<b>0.00734</b>	67.8±2.0	27.6±3.2	<b>0.00406</b>	76.3±3.3	9.4±1.4	<b>0.00091</b>
S+G <sub>2</sub> /M	20.2±1.3	6.4±0.8	<b>0.00384</b>	11.3±1.1	12.0±0.6	0.13694	29.6±2.5	68.5±3.7	<b>0.00632</b>	20.0±2.5	87.5±1.3	<b>0.00046</b>
<i>48 h</i>												
Sub-G <sub>1</sub>	3.2±0.5	75.3±2.1	<b>0.00032</b>	4.4±1.4	59.2±3.5	<b>0.00196</b>	3.3±1.1	6.0±2.3	0.05624	4.6±0.7	5.7±1.5	0.09568
G <sub>1</sub>	78.7±1.8	17.1±1.7	<b>0.00024</b>	84.1±3.6	34.3±1.9	<b>0.00299</b>	67.7±2.1	19.8±3.1	<b>0.00292</b>	76.3±3.2	8.8±2.5	<b>0.00046</b>
S+G <sub>2</sub> /M	18.1±1.4	7.6±3.1	<b>0.00942</b>	11.5±2.6	6.5±1.7	<b>0.04318</b>	28.9±2.8	74.2±4.0	<b>0.00393</b>	19.0±4.0	85.5±3.5	<b>0.00033</b>

\*P-value was obtained by a paired Student's *t*-test between the data from untreated (control) and PKC412-treated (PKC412) cells (*n* = 3). Data are the means ± s.d. of three independent experiments. Bold values indicate *P* < 0.05. \*The proportion of cells in each phase of the cell cycle was calculated with the ModFitLT 2.0 program.

in MOLM13 and MV4-11, and increased in THP-1 and U937 after treatment with the drug. The inhibition of CDC2 kinase activity may underlie PKC412-induced G<sub>2</sub> arrest of THP-1 and U937 cells.

As Myt-1 kinase is responsible for CDC2 phosphorylation at tyrosine-15 (Galaktionov *et al.*, 1995), we examined the activation status of Myt-1 in these cells by immunoblotting with an antibody specifically recognizing the inactive/phosphorylated species of Myt-1. Consistent with the phosphorylation status of CDC2, Myt-1 was active (underphosphorylated) in AML cell lines with FLT3-ITD and inactive (phosphorylated) in AML cell lines without FLT3-ITD before treatment with PKC412 (Figure 3a). Myt-1 became phosphorylated and thereby inactivated by PKC412 in the former, whereas it became dephosphorylated and thereby activated in the latter, leading to the increased phosphorylation of CDC2. It is of note that Wee1, another kinase involved in tyrosine-15 phosphorylation, was below the detection limit in FLT3 mutation-positive leukemic cells as previously described (Neben *et al.*, 2005).

Next, we investigated the effects of PKC412 on the activity and intracellular localization of CDC25c, which activates CDC2 by removing phosphates from tyrosine-15. CDC25c was phosphorylated at serine-216 in untreated MOLM13 and MV4-11 cells, and was dephosphorylated by PKC412 (Figure 3a). In contrast, PKC412 increased the serine-216 phosphorylation of CDC25c in THP-1 and U937 cells. Upon phosphorylation at serine-216, CDC25c binds to 14-3-3 proteins and is translocated from the nucleus to the cytoplasm (Lopez-Girona *et al.*, 1999). We therefore confirmed the cytoplasmic sequestration of CDC25c phosphorylated at serine-216 using immunocytochemistry. As shown in Figure 3b, CDC25c was mostly retained in the cytoplasm in untreated MOLM13 cells, and was translocated to the nucleus after treatment with PKC412. In contrast, CDC25c was distributed throughout the entire cells in untreated U937 cells, and became

sequestered in the cytoplasm and thus inactivated by the addition of PKC412. These observations are fully consistent with the pattern of serine-216 phosphorylation shown in Figure 3a. Furthermore, we demonstrated the binding of phosphorylated CDC25c to 14-3-3 proteins in cytoplasm using confocal microscopy. As shown in Figure 3c, phosphorylated CDC25c colocalized with 14-3-3 in untreated MV4-11 cells, and the interaction was dissociated after culture with PKC412. In U937 cells, PKC412 increased the amounts of phosphorylated CDC25c, which translocated from the nucleus and bound to 14-3-3 proteins in the cytoplasm. These results at least partly explain why PKC412 arrests cells in the G<sub>2</sub> phase of the cell cycle exclusively in AML cell lines without FLT3 mutations.

*PKC412-induced apoptosis of AML cell lines with FLT3 mutations is mediated via selective phosphorylation of Bad at serine-128*

Finally, we attempted to clarify the molecular mechanisms by which only AML cells with FLT3 mutations underwent apoptosis in the presence of PKC412. To this end, we screened for the expression of proapoptotic members of the Bcl-2 family by immunoblotting. As the expression of Bax and Bak was constitutive and unaffected by PKC412 in four AML cell lines (data not shown), we focused on BH3-only members of the Bcl-2 family, direct inducers of apoptosis (Galonek and Hardwick, 2006; Green, 2006). Among BH3-only proteins examined, only Bad was moderately expressed, and Bim, Bid, Puma and Noxa were undetectable in AML cell lines used in this study (data not shown). As PKC412 did not change the abundance of Bad protein, we examined the phosphorylation status of Bad using phosphorylation site-specific antibodies. It has been shown that Bad phosphorylation at various residues represents a checkpoint for the cell fate decision. For instance, CDC2 enhances the proapoptotic ability of



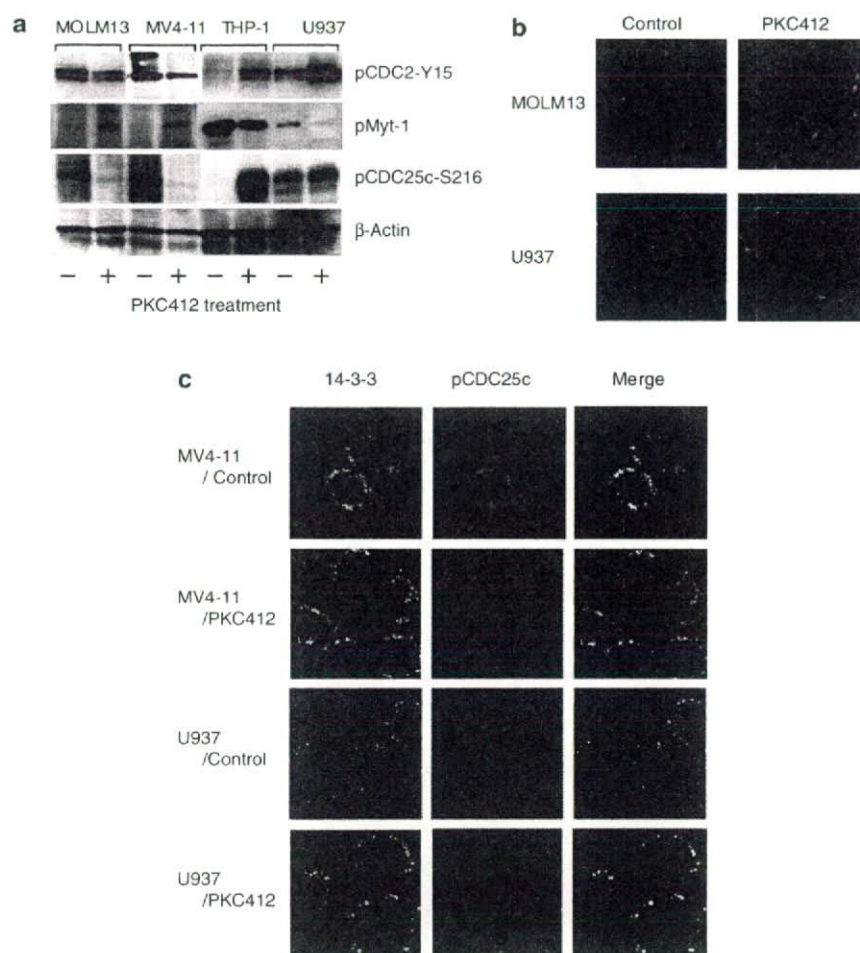


**Figure 3** PKC412 differentially modulates CDC2 phosphorylation in acute myeloblastic leukemia (AML) cell lines depending on the presence of FLT3 mutations. (a) Whole cell lysates were prepared from AML cell lines before (–) and after (+) culture with 100 nM PKC412 for 24 h, and subjected to immunoblot analysis for the indicated proteins. (b) Intracellular localization of CDC25c was examined by immunocytochemistry in MOLM13 and U937 cells cultured in the absence (control) or presence (PKC412) of 100 nM PKC412 for 24 h. After being fixed, cells were stained with an anti-CDC25c monoclonal antibody and Alexa 488-conjugated goat antibody to mouse immunoglobulin. Original magnification is  $\times 600$  for all panels. (c) Colocalization of CDC25c and 14-3-3 proteins was examined by confocal microscopy in MV4-11 and U937 cells cultured in the absence (control) or presence (PKC412) of 100 nM PKC412 for 24 h. After being fixed, cells were stained with antibodies against 14-3-3 proteins and CDC25c phosphorylated at serine 216, followed by incubation with Alexa 488-conjugated goat antibody to mouse immunoglobulin and Cy3-conjugated goat antibody to rabbit immunoglobulin. Original magnification is  $\times 600$  for all panels. Data shown are representative of multiple independent experiments.

Bad by promoting serine-128 phosphorylation and mitochondrial translocation of Bad (Konishi *et al.*, 2002). In contrast, Akt promotes cell survival by phosphorylating Bad at serine-136, which provides a canonical binding site for 14-3-3 proteins to disrupt interaction with Bcl-2/Bcl-x on mitochondrial membranes (Zha *et al.*, 1996). Bad was phosphorylated at serine-136 and was inactive in untreated AML cells (Figure 4a, upper panel). Marginal levels of phosphorylation at serine-128 were observed in THP-1 and U937 cells, which may be due to the hyperactivation of CDC2. PKC412 induced Bad phosphorylation at serine-128 selectively in AML cell lines with FLT3-ITD along with dephosphorylation at serine-136 (Figure 4a, lower panel). AML cell lines with wild-type FLT3 did not

show serine-128 phosphorylation. Next, we examined the intracellular localization of Bad using confocal microscopy. In untreated MV4-11 and U937 cells, Bad was distributed throughout the cytoplasm and did not colocalize with mitochondria (Figure 4b, Control). PKC412 induced the translocation of Bad to the mitochondria in MV4-11 cells but not in U937 cells (Figure 4b, PKC412). Intracellular localization of Bad is fully compatible with the alteration of site-specific phosphorylation of Bad, and at least partly explains the selective induction of apoptosis in AML cells with FLT3 mutations by PKC412.

Next, we determined the effects of PKC412 on the expression of antiapoptotic members of the Bcl-2 family. Immunoblot analyses revealed that AML cell lines used



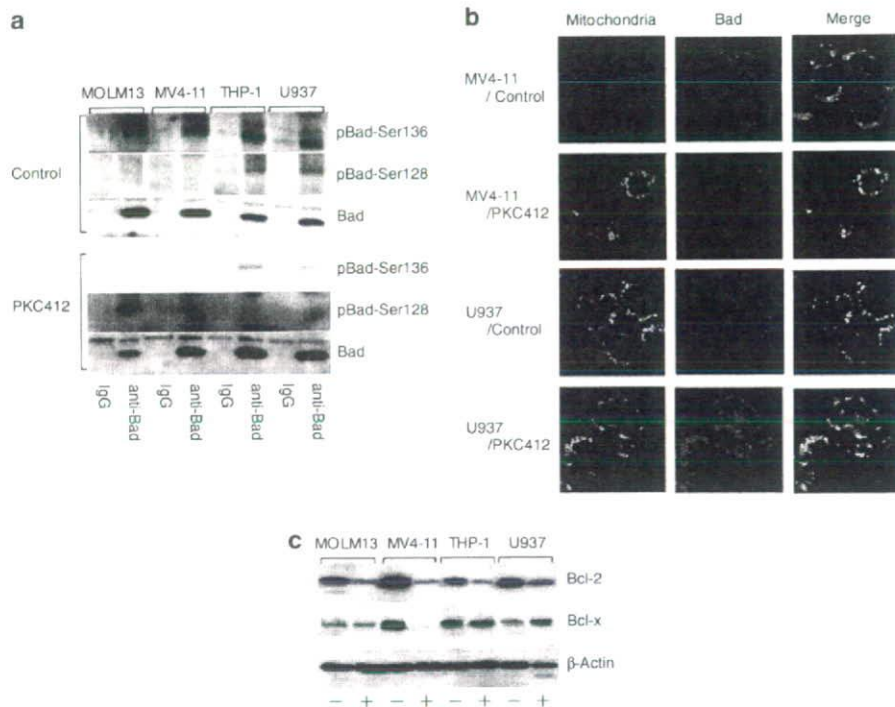


**Figure 4** PKC412-induced apoptosis of acute myeloblastic leukemia (AML) cell lines with FLT3 mutations is mediated via phosphorylation of Bad at serine-128. **(a)** Whole cell lysates were prepared from AML cell lines cultured in the absence (control) or presence (PKC412) of 100 nM PKC412 for 24 h, and subjected to immunoprecipitation with either anti-Bad monoclonal antibody (anti-Bad) or mouse IgG (IgG). Immunoprecipitants were resolved on 12% acrylamide gels, followed by immunoblotting with polyclonal antibodies against Bad phosphorylated at serine-136, Bad phosphorylated at serine-128 and Bad. **(b)** For *in situ* visualization of Bad, we used anti-Bad polyclonal antibody and Cy3-conjugated goat antibody to rabbit immunoglobulin as primary and secondary antibodies, respectively. For co-labeling of mitochondria, we used a combination of anti-human mitochondria monoclonal antibody and Alexa 488-conjugated goat antibody to mouse immunoglobulin. **(c)** Protein samples in **(a)** were subjected to immunoblot analyses for Bcl-2, Bcl-x and  $\beta$ -actin (loading control). Data shown are representative of multiple independent experiments.

in this study expressed Bcl-2 and Bcl-x but not Mcl-1 and Bcl-w (data not shown). As shown in Figure 4c, Bcl-2 was readily downregulated by PKC412 in all four cell lines. The effects of PKC412 on Bcl-x expression were variable, suggesting that downregulation of Bcl-2 and Bcl-x is not a primary determinant of the sensitivity of AML cells to PKC412. However, it is possible that the reduced levels of Bcl-2 expression cooperate with the activation of Bad to enhance apoptosis in PKC412-treated MOLM13 and MV4-11 cells.

*PKC412 induces apoptosis in primary AML cells with FLT3 mutations via the CDC2-Bad pathway*

To testify the clinical relevance of our findings, we carried out the same experiments using primary AML cells from three patients with AML carrying FLT3-ITD. As shown in Figure 5a, PKC412 induced apoptosis with a decrease in the fraction of cells in the S phase in two cases and G<sub>1</sub> arrest with a moderate degree of apoptosis in one case. The effects of the drug on the phosphorylation status of FLT3, CDC2, Myt-1, CDC25c and Bad were almost identical to those observed in MOLM13 and MV4-11 cell lines (Figure 5b). These results indicate that our findings are not only valid in the cell line models, but have more general meanings.

**Discussion**

In this study, we obtained a clue pertinent to the molecular basis of the synergism and antagonism of PKC412 with other antileukemic agents. PKC412 alone induced G<sub>2</sub> arrest but not apoptosis in AML cell lines without aberrant FLT3 activation (THP-1 and U937) at a clinically achievable concentration. Because of the ability to cause G<sub>2</sub> arrest, PKC412 is synergistic with drugs that are active in the G<sub>2</sub>/M phase, such as colchicine, in these cell lines. This may be an important advantage for the usage of PKC412 over other FLT3 inhibitors, because such effects have not been demonstrated with other FLT3 inhibitors (Levis *et al.*, 2004; Yee *et al.*, 2004). For the same reason, PKC412 may be antagonistic with drugs that synchronize target cells in late G<sub>1</sub> to early S phase, such as aphidicolin, in FLT3 mutation-negative leukemias. In contrast, PKC412-induced massive apoptosis without markedly affecting cell cycle patterns in AML cell lines harboring FLT3 mutations, which may underlie the synergism of PKC412 with most antileukemic agents.

Next, we attempted to elucidate the underlying mechanisms whereby PKC412 differentially affects the cell cycle distribution depending on the presence of FLT3 mutations. We obtained evidence suggesting that



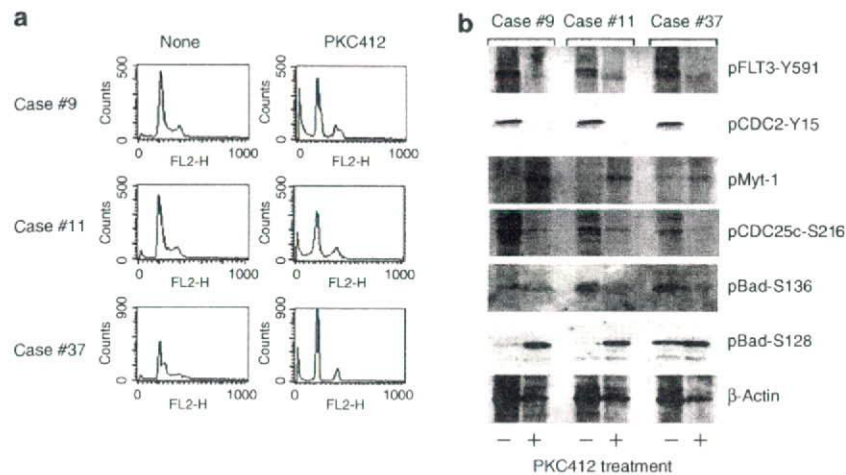


**Figure 5** PKC412 induces apoptosis and cell cycle alterations in primary acute myeloblastic leukemia (AML) cells via the CDC2-Bad pathway. Bone marrow mononuclear cells from patients with AML carrying FLT3-ITD were cultured in the absence (none) or presence (PKC412) of 100 nM PKC412 for 24 h, and subjected to cell cycle analysis (a) and immunoblotting (b).

the cell cycle effect is mediated through the modulation of CDC2 activity by PKC412. The kinase activity of CDC2 is regulated by the opposing effects of specific kinases (Myt-1 and Wee1) and a specific phosphatase (CDC25c) on tyrosine-15, an ATP-binding site of CDC2 (Galaktionov *et al.*, 1995; Watanabe *et al.*, 1995). In untreated AML cell lines harboring FLT3-ITD, CDC2 was found to be at least partially inactivated by phosphorylation at tyrosine-15. This may be attributable to FLT3-ITD-mediated activation of Myt-1 kinase and inactivation of CDC25c by serine-216 phosphorylation and subsequent binding to 14-3-3 proteins. We are now trying to elucidate the signaling pathways of FLT3-ITD causing these changes. The partial inactivation of CDC2 may underlie the observation that AML cells with FLT3-ITD grow slower than those with wild-type FLT3. PKC412 reversed this process and activated CDC2 by promoting Myt-1 inactivation and facilitating nuclear translocation of CDC25c. In AML cells without FLT3-ITD, CDC2 is mostly in an active conformation and allows rapid cell cycling. PKC412 seems to inhibit CDC2 activity through CDC25c inactivation, which results in G<sub>2</sub> arrest. Although the precise mechanisms underlying this phenomenon are at present unknown, similar observations have been reported in non-small cell lung cancer and glioblastoma (Ikegami *et al.*, 1996; Begemann *et al.*, 1998).

Finally, we went on to identify target molecules responsible for selective induction of apoptosis in PKC412-treated AML cells with FLT3 mutations. To this end, we investigated the expression and function of Bcl-2 family proteins. Apoptotic cell death usually occurs through mitochondrial outer membrane permeabilization (MOMP), which is controlled by the balance between pro- and antiapoptotic members of the Bcl-2 family. Bad is a member of the BH3-only subfamily, and is known to promote MOMP by activating membrane-anchored proapoptotic Bcl-2 family proteins Bax and Bak (Galonek and Hardwick, 2006; Green, 2006). The

function of Bad is tightly regulated by phosphorylation. For instance, the PI3 kinase-Akt pathway mediates phosphorylation of Bad at serine-136 and abrogates its proapoptotic activity (Zha *et al.*, 1996). It is well known that FLT3-ITD phosphorylates Bad through the Akt pathway and suppresses apoptosis of hematopoietic stem cells, which contribute to the development of leukemia (Kim *et al.*, 2006). In contrast, serine-128 phosphorylation promotes apoptosis in primary neurons by antagonizing survival functions of growth factors (Konishi *et al.*, 2002). Serine-128 phosphorylation is shown to be catalysed by CDC2 and c-Jun N-terminal kinase (Donovan *et al.*, 2002). Our results suggest that PKC412 causes phosphorylation of Bad at serine-128 via CDC2 activation along with dephosphorylation at serine-136 via blocking FLT3-ITD signaling, which results in apoptosis of AML cells with FLT3 mutations. In AML cells without FLT3-ITD, Bad phosphorylation at serine-128 did not occur because of PKC412-mediated inactivation of CDC2. Although serine-136 was dephosphorylated in some degree, these cells did not undergo apoptosis in response to PKC412. This is in line with a previous report that dephosphorylation of Bad is not sufficient and downregulation of Bcl-x is necessary for the induction of apoptosis (Yang *et al.*, 2005). In addition, Bcl-x inhibits CDC2 kinase activity at the G<sub>2</sub>/M checkpoint by direct binding and causes G<sub>2</sub> arrest (Schmitt *et al.*, 2007). As Bcl-x was not downregulated in PKC412-treated THP-1 and U937 cells, it is possible that Bcl-x serves as an additional factor to determine the responses to PKC412.

**Materials and methods**

*Reagents*

PKC412 was purchased from LC Laboratories (Woburn, MA, USA), dissolved in dimethyl sulfoxide and stored at -20 °C until use.



#### Cells and cell culture

We used four human AML cell lines, that is, MOLM13, derived from a patient with acute monocytic leukemia (AMoL) carrying t(9;11); MV4-11, derived from a patient with AMoL carrying t(4;11); THP-1 and U937, derived from patients with AMoL without FLT3 mutations. MV4-11, THP-1 and U937 were purchased from the American Type Culture Collection (Manassas, VA, USA), and MOLM13 was provided by Dr Yoshinobu Matsuo (Grandsoul Research Institute for Immunology, Nara, Japan). These cell lines were maintained in RPMI1640 medium supplemented with 10% fetal bovine serum. Primary AML cells were isolated from the bone marrow of patients at the time of diagnostic procedure. Informed consent was obtained in accordance with the Declaration of Helsinki, and the protocol was approved by the institutional review board. The presence of FLT3-ITD was examined as described by Kiyoi *et al.* (1997).

#### Flow cytometric analysis

The cell cycle profile was obtained by staining DNA with Vindelov's solution (0.04 mg ml<sup>-1</sup> propidium iodide in 5 mM Tris-HCl, 5 mM NaCl and 0.005% nonidet P-40) in preparation for flow cytometry. The size of the sub-G<sub>1</sub>, G<sub>0</sub>/G<sub>1</sub> and S+G<sub>2</sub>/M fractions was calculated as a percentage by analysing DNA histograms with the ModFitLT 2.0 program (Verity Software, Topsham, ME, USA). Surface marker analysis was carried out according to the standard method.

#### Immunocytochemistry

After collecting on glass slides using a Cytospin centrifugator (Shandon Scientific, Cheshire, England), cells were fixed in 4% paraformaldehyde in phosphate-buffered saline, and stained with a rabbit antitubulin polyclonal antibody (Sigma, St Louis, MO, USA) and Alexa 488-conjugated goat antibody to rabbit immunoglobulin (Molecular Probes, Eugene, OR, USA) as primary and secondary antibodies, respectively. Finally, nuclear DNA was stained with 100 ng ml<sup>-1</sup> propidium iodide in phosphate-buffered saline for 5 min.

#### Detection of apoptosis

Apoptosis was detected *in situ* by the TUNEL (TdT-mediated dUTP-biotin nick end labeling) method using MEBSTAIN apoptosis kit (MBL International, Woburn, MA, USA). In brief, cells were fixed on glass slides as described above, and treated with terminal deoxynucleotidyl transferase (TdT) in the presence of biotin-dUTP to label 3'-ends of fragmented DNA. The labeled ends were visualized with avidin-conjugated

fluorescein isothiocyanate (FITC). Finally, intact DNA was counterstained with propidium iodide.

#### Confocal laser microscopy

Confocal microscopic analysis was performed using the following antibodies: anti-CDC25c (C2-2; BD Pharmingen, San Jose, CA, USA), antiphosphorylated CDC25c at serine-216 (no. 4901; Cell Signalling Technology, Beverly, MA, USA), anti-human 14-3-3 (C23-1; BD Pharmingen), anti-Bad (no. 9292; Cell Signalling Technology) and anti-human mitochondria (AE-1; Leinco Technologies Inc., St Louis, MO, USA). We used Alexa 488-conjugated goat antibody to mouse immunoglobulin (Molecular Probes) and Cy3-conjugated goat antibody to rabbit immunoglobulin (Amersham Pharmacia Biotech, Piscataway, NJ, USA) as secondary antibodies.

#### Immunoprecipitation and immunoblotting

Immunoprecipitation and immunoblotting were carried out according to the standard methods using the following antibodies: anti-FLT3 (8F2; Santa Cruz Biotechnology, Santa Cruz, CA, USA), antiphosphorylated FLT3 at tyrosine-591 (no. 3461; Cell Signalling Technology), antiphosphorylated protein kinase C (pan) at serine-660 (no. 9371; Cell Signalling Technology), antiphosphorylated c-Kit at tyrosine-719 (no. 3391; Cell Signalling Technology), antiphosphorylated PDGF receptor  $\beta$  at tyrosine-751 (no. 3161; Cell Signalling Technology), antiphosphorylated CDC2 at tyrosine-15 (no. 9111; Cell Signalling Technology), anti-Bad monoclonal (clone 48; BD Transduction Laboratories, San Jose, CA, USA), anti-Bad polyclonal (no. 9292; Cell Signalling Technology), antiphosphorylated Bad at serine-136 (no. 9295; Cell Signalling Technology), antiphosphorylated Bad at serine-128 (AB3567; Chemicon International, Temecula, CA, USA), anti-Bcl-2 (clone 4D7; BD Transduction Laboratories), anti-Bcl-x (clone 44; BD Transduction Laboratories) and anti- $\beta$ -actin (C4; ICN Biomedicals, Aurora, OH, USA).

#### Acknowledgements

This work was supported in part by the High-Tech Research Center Project for Private Universities: Matching Fund Subsidy from MEXT 2002–2006, and grants from the Vehicle Racing Commemorative Foundation and Sankyo Foundation of Life Science (to YF). JK is a winner of the Jichi Medical School Young Investigator Award. TW is a winner of the Jichi Medical School Graduate Student Award.

#### References

- Begemann M, Kashimawo SA, Heitjan DF, Schiff PB, Bruce JN, Weinstein IB. (1998). Treatment of human glioblastoma cells with the staurosporine derivative CGP 41251 inhibits CDC2 and CDK2 kinase activity and increases radiation sensitivity. *Anticancer Res* **18**: 2275–2282.
- Donovan N, Becker EB, Konishi Y, Bonni A. (2002). JNK phosphorylation and activation of BAD couples the stress-activated signaling pathway to the cell death machinery. *J Biol Chem* **277**: 40944–40949.
- Furukawa Y, Vu HA, Akutsu M, Odgerel T, Izumi T, Tsunoda S *et al.* (2007). Divergent cytotoxic effects of PKC412 in combination with conventional antileukemic agents in FLT3 mutation-positive versus negative leukemia cell lines. *Leukemia* **21**: 1005–1014.
- Galaktionov K, Jessus C, Beach D. (1995). Raf1 interaction with Cdc25 phosphatase ties mitogenic signal transduction to cell cycle activation. *Genes Dev* **9**: 1046–1058.
- Galonek HL, Hardwick JM. (2006). Upgrading the bcl-2 network. *Nat Cell Biol* **12**: 1317–1319.
- Gilliland DG, Griffin JD. (2002). The roles of FLT3 in hematopoiesis and leukemia. *Blood* **100**: 1532–1542.
- Green DR. (2006). At the gates of death. *Cancer Cell* **9**: 328–330.
- Griffin JD. (2004). FLT3 tyrosine kinase as a target in acute leukemias. *Hematol J* **5**: 188–190.
- Ikegami Y, Yano S, Nakao K. (1996). Effects of the new selective protein kinase C inhibitor 4'-N-benzoyl staurosporine on cell cycle distribution and growth inhibition in human small cell lung cancer cells. *Arzneimittelforschung* **46**: 201–204.
- Kelly LM, Liu Q, Kutok JL, Williams IR, Boulton CL, Gilliland DG. (2002). FLT3 internal tandem duplication mutations associated with human acute myeloid leukemias induce myeloproliferative disease in a murine bone marrow transplant model. *Blood* **99**: 310–318.



- Kim KT, Levis M, Small D. (2006). Constitutively activated FLT3 phosphorylates BAD partially through pim-1. *Br J Haematol* **134**: 500–509.
- Kiyoi H, Naoe T, Yokota S, Nakao M, Minami S, Kuriyama K *et al.* (1997). Internal tandem duplication of FLT3 associated with leukocytosis in acute promyelocytic leukemia. *Leukemia* **11**: 1447–1452.
- Konishi Y, Lehtinen M, Donovan N, Bonni A. (2002). Cdc2 phosphorylation of BAD Links the cell cycle to the cell death machinery. *Mol Cell* **9**: 1005–1016.
- Levis M, Pham R, Smith BD, Small D. (2004). *In vitro* studies of a FLT3 inhibitor combined with chemotherapy: sequence of administration is important to achieve synergistic cytotoxic effects. *Blood* **104**: 1145–1150.
- Levis M, Small D. (2005). FLT3 tyrosine kinase inhibitors. *Int J Hematol* **82**: 100–107.
- Lopez-Girona A, Furnari B, Mondesert O, Russell P. (1999). Nuclear localization of Cdc25 is regulated by DNA damage and a14-3-3 protein. *Nature* **397**: 172–175.
- Lyman SD, James L, Vanden Bos T, de Vries P, Brasel K, Gliniak B *et al.* (1993). Molecular cloning of a ligand for the flt3/flk-2 tyrosine kinase receptor: a proliferative factor for primitive hematopoietic cells. *Cell* **75**: 1157–1167.
- Neben K, Schnittger S, Bross B, Tews B, Kokocinski F, Haferlach T *et al.* (2005). Distinct gene expressions patterns associated with FLT3- and NRAS- activating mutations in acute myeloid leukemia with normal karyotype. *Oncogene* **24**: 1580–1588.
- Propper DJ, McDonald AC, Man A, Thavasu P, Balkwill F, Braybrooke JP *et al.* (2001). Phase I and pharmacokinetic study of PKC412, an inhibitor of protein kinase C. *J Clin Oncol* **19**: 1485–1492.
- Quentmeier H, Reinhardt J, Zaborski M, Drexler HG. (2003). FLT3 mutations in acute myeloid leukemia cell lines. *Leukemia* **17**: 120–124.
- Schmitt E, Beauchemin M, Bertrand R. (2007). Nuclear colocalization and interaction between bcl-xL and cdk1 (cdc2) during G2/M cell-cycle checkpoint. *Oncogene* **26**: 5851–5865.
- Small D, Levenstein M, Kim E, Carow C, Amin S, Rockwell P *et al.* (1994). STK-1, the human homolog of Flk-2/Flt-3, is selectively expressed in CD34<sup>+</sup> human bone marrow cells and is involved in the proliferation of early progenitor/stem cells. *Proc Natl Acad Sci USA* **91**: 459–463.
- Stone RM, DeAngelo DJ, Klimek V, Galinsky I, Estey E, Nimer SD *et al.* (2005). Patients with acute myeloid leukemia and an activating mutation in FLT3 respond to a small-molecule FLT3 tyrosine kinase inhibitor, PKC412. *Blood* **105**: 54–60.
- Watanabe N, Broome M, Hunter T. (1995). Regulation of the human Wee1 CDK tyrosine 15 kinase during cell cycle. *EMBO J* **14**: 1878–1891.
- Weisberg E, Boulton C, Kelly LM, Manley P, Fabbro D, Meyer T *et al.* (2002). Inhibition of mutant FLT3 receptors in leukemia cells by the small molecule tyrosine kinase inhibitor PKC412. *Cancer Cell* **1**: 433–443.
- Yang X, Lui L, Sternberg D, Tang L, Galinsky I, DeAngelo D *et al.* (2005). The FLT3 internal tandem duplication mutation prevents apoptosis in interleukin 3-deprived BaF3 cells due to protein kinase A and ribosomal S6 Kinase 1-mediated BAD phosphorylation at serine 112. *Cancer Res* **65**: 7338–7347.
- Yao Q, Nishiuchi R, Li Q, Kumar AR, Hudson WA, Kersey JH. (2003). FLT3 expressing leukemias are selectively sensitive to inhibitors of the molecular chaperone heat shock protein 90 through destabilization of signal transduction-associated kinases. *Clin Cancer Res* **9**: 4483–4493.
- Yee KW, Schittenhelm M, O'Farrell AM, Town AR, McGreevey L, Bainbridge T *et al.* (2004). Synergistic effect of SU11248 with cytarabine or daunorubicin on FLT3 ITD-positive leukemic cells. *Blood* **104**: 4202–4209.
- Zha J, Harada H, Yang F, Jockel J, Korsmeyer SJ. (1996). Serine phosphorylation of death agonist Bad in response to survival factor results in binding to 14-3-3 not BCL-XL. *Cell* **87**: 619–628.

Supplementary Information accompanies the paper on the Oncogene website (<http://www.nature.com/onc>).



# Transcriptional Modulation Using HDACi Depsipeptide Promotes Immune Cell-Mediated Tumor Destruction of Murine B16 Melanoma

Takashi Murakami<sup>1</sup>, Atsuko Sato<sup>1,2</sup>, Nicole A.L. Chun<sup>1</sup>, Mayumi Hara<sup>1</sup>, Yuki Naito<sup>1</sup>, Yukiko Kobayashi<sup>2,3</sup>, Yasuhiko Kano<sup>4</sup>, Mamitaro Ohtsuki<sup>2</sup>, Yusuke Furukawa<sup>3</sup> and Eiji Kobayashi<sup>1</sup>

With melanoma, as with many other malignancies, aberrant transcriptional repression is a hallmark of refractory cancer. To restore gene expression, use of a histone deacetylase inhibitor (HDACi) is expected to be effective. Our recent DNA micro-array analysis showed that the HDACi depsipeptide (FK228) significantly enhances gp100 antigen expression. Herein, we demonstrate that depsipeptide promotes tumor-specific T-cell-mediated killing of B16/F10 murine melanoma cells. First, by a quantitative assay of caspase-3/7 activity, a sublethal dose of depsipeptide was determined (ED50: 5 nM), in which p21<sup>Waf1/Cip1</sup> and Fas were sufficiently evoked concomitantly with histone H3 acetylation. Second, the sublethal dose of depsipeptide treatment with either a recombinant Fas ligand or tumor-specific T cells synergistically enhanced apoptotic cell death in B16/F10 cells *in vitro*. Furthermore, we found that T-si peptide increased levels of perforin in T cells. Finally, *in vivo* metastatic growth of B16/F10 in the lung was significantly inhibited by a combination of depsipeptide treatment and immune cell adoptive transfer from immunized mice using irradiated B16 cells and gp100-specific (Pmel-1) TCR transgenic mice ( $P < 0.05$ , vs cell transfer alone). Consequently, employment of a transcriptional modulation strategy using HDACis might prove to be a useful pretreatment for human melanoma immunotherapy.

*Journal of Investigative Dermatology* (2008) **128**, 1506–1516; doi:10.1038/sj.jid.5701216; published online 10 January 2008

## INTRODUCTION

Great efforts have been made in the field of tumor immunology, and attempts to enhance cellular immune responses have used various cancer antigens and immunizing vectors (Rosenberg, 2004; Gattinoni *et al.*, 2006). Although these strategies allow for the generation of immune T cells that recognize antigenic peptides present on tumor cells, the regression of growing tumors in patients treated with active immunization has been sporadic and rare (Rosenberg *et al.*, 2004). In fact, a variety of factors that limit tumor regression despite the *in vivo* generation of antitumor T cells have been reported (Rosenberg and Dudley, 2004), and it is therefore necessary to overcome many tumor and lymphocyte factors

that cause the tumor-escape mechanisms. Targeting key survival pathways in tumor cells, particularly those that allow cancer cells to prevent host immune attacks, is an attractive approach when aiming for an increase in the effectiveness of cancer immunotherapy.

There are emerging data suggesting that aberrant transcriptional repression of genes to control cell growth and differentiation is a hallmark of malignancy (Herman and Baylin, 2003). With melanoma, as with many other cancers, alteration of histone deacetylases (HDACs) underlies the transcriptional repression (Klisovic *et al.*, 2003; Kobayashi *et al.*, 2006). Thus, blockade of HDACs might restore global gene expression in cancer cells, making them sensitive to cell cycle arrest, differentiation, and apoptotic cell death (Johnstone and Licht, 2003; Minucci and Pelicci, 2006). The action mode of histone deacetylase inhibitors (HDACis), as the transcriptional modulator, differs from that of other anti-cancer agents (Marks *et al.*, 2001), and HDACis are expected to be effective for many cancer types that resist conventional chemotherapy (Marks *et al.*, 2001; Minucci and Pelicci, 2006). Indeed, HDACis have shown cytotoxicity in a variety of human and rodent cancer cells *in vitro* and *in vivo* (Hoshikawa *et al.*, 1994), some of which are being tested in clinical studies (Minucci and Pelicci, 2006).

Depsipeptide (also referred to as FK228 and FR901228) may be considered a promising HDACi for human melanoma. It was originally isolated from *Chromobacterium violaceum* (no. 968) as a compound that reversed the

<sup>1</sup>Division of Organ Replacement Research, Center for Molecular Medicine, Jichi Medical University, Shimotuke, Tochigi, Japan; <sup>2</sup>Department of Dermatology, Jichi Medical University, Shimotuke, Tochigi, Japan; <sup>3</sup>Division of Stem Cell Regulation, Center for Molecular Medicine, Jichi Medical University, Shimotuke, Tochigi, Japan and <sup>4</sup>Division of Medical Oncology, Tochigi Cancer Center, Utsunomiya, Tochigi, Japan

Correspondence: Dr Takashi Murakami, Division of Organ Replacement Research, Center for Molecular Medicine, Jichi Medical University, 3311-1 Yakushiji, Shimotuke, Tochigi 329-0498, Japan.  
E-mail: takmu@jichi.ac.jp

Abbreviations: CTL, cytotoxic T lymphocyte; FasL, Fas ligand; FCS, fetal calf serum; HDAC, histone deacetylase; HDACi, histone deacetylase inhibitor; MHC, major histocompatibility complex; PE, phycoerythrin; RT-PCR, reverse transcription-PCR; s.c., subcutaneous

Received 7 May 2007; revised 14 September 2007; accepted 3 November 2007; published online 10 January 2008



malignant phenotype of H-ras-transformed fibroblasts by blocking the p21<sup>ras</sup>-mediated signal transduction pathway (Ueda *et al.*, 1994a,b). Depsipeptide suppressed cell proliferation and induced apoptosis in human uveal melanoma cell lines at relatively high doses (Klisovic *et al.*, 2003) and produced substantial therapeutic effects on various malignancies (Minucci and Pelicci, 2006). In our previous study to determine the molecular basis of its cytotoxic effect, depsipeptide suppressed the Ras-mitogen-activated protein kinase signaling pathway through Rap1 upregulation, leading to apoptosis in human melanoma cells (Kobayashi *et al.*, 2006). Herein, we show that depsipeptide sensitized poorly immunogenic murine B16 melanoma cells to the Fas ligand and that a limited dose of depsipeptide suppressed *in vivo* growth of B16/F10 in combination with adoptive immune cell transfer therapy. Consequently, a transcriptional modulation strategy using HDACis might prove to be a useful adjunct in human immunotherapy strategies against cancer.

**RESULTS**

**Depsipeptide enhances expression of gp100/pmel17 melanoma antigen in melanoma cell lines**

Our recent DNA micro-array study revealed that the HDACi depsipeptide markedly enhanced mRNA expression of gp100/pmel17 melanoma antigen in MM-LH human melanoma cells (15-fold increase) (Kobayashi *et al.*, 2006). Thus, we initially hypothesized that gp100/pmel17 would be a potential target of depsipeptide in human melanoma cells. The expression of gp100/pmel17 in human melanoma cell lines was examined

by reverse transcription-PCR (RT-PCR) (Figure 1a). All melanoma cell lines examined showed strong enhancement of gp100/pmel17 mRNA expression after exposure to depsipeptide (10 nM) for 16 hours, whereas normal healthy melanocytes were not affected by the same dose of depsipeptide. The expression of gp100/pmel17 by depsipeptide was moderately enhanced in murine B16/F10 melanoma cells.

To characterize the effects of depsipeptide in a murine model of melanoma, we examined the ability of depsipeptide to induce histone acetylation in B16/F10 cells (Figure 1b). Basal acetylation of histone H3 (lysine residue 9) was detected, and subsequent experiments revealed that the acetylation level of histone H3 (lysine residues 9 and 18) increased significantly after a 24 hour exposure to 1–10 nM depsipeptide. Furthermore, major histocompatibility complex (MHC) class I (H2-D<sup>b</sup>) and Fas (CD95) death receptor expression were enhanced in B16/F10 cells exposed to depsipeptide (Figure 1c). In human melanoma cell lines, to depsipeptide resulted in moderately enhanced MHC class I expression but not Fas expression (Figure S1). Thus, a 1–10 nM depsipeptide dose could sufficiently modulate murine B16/F10 melanoma cells within 16 hours *in vitro*, suggesting that a limited dose of depsipeptide may be effective for recognition and sensitization of immune cell-mediated tumor destruction in mice.

**A limited dose of depsipeptide moderately induces apoptosis and cell cycle arrest in murine B16 melanoma cells**

We have shown previously that depsipeptide induces apoptotic cell death in human melanoma cell lines (Kobayashi

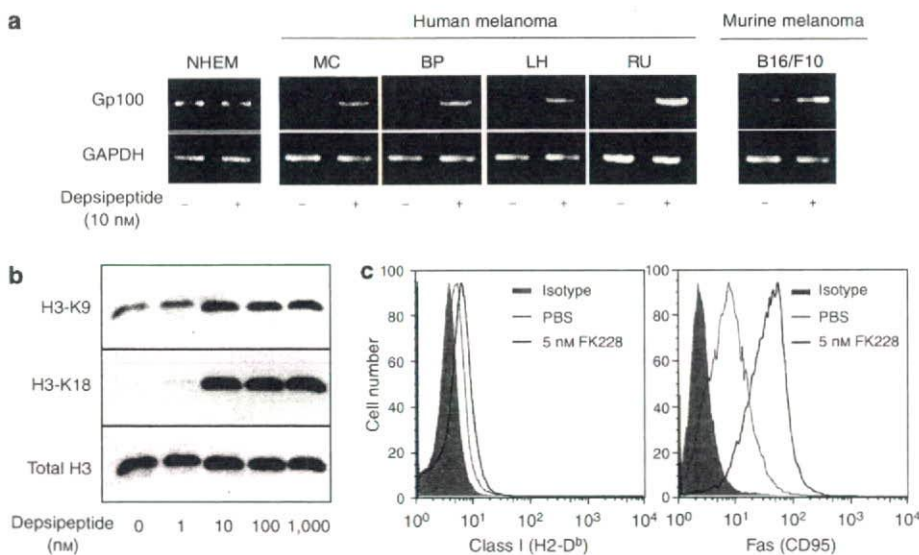


**Figure 1. Depsipeptide enhances expression of gp100/pmel17 melanoma antigen.** (a) RT-PCR analysis of gp100/pmel17 transcript. Total RNA was extracted from each melanoma cell line after exposure to depsipeptide (10 nM) for 16 hours. PCR was performed with primers as described in Materials and Methods. GAPDH, glyceraldehyde-3-phosphate dehydrogenase (as an internal control); NHEM, normal healthy melanocytes; MC (RPM-MC), BP (MM-BP), LH (MM-LH), and RU (MM-RU) are human melanoma cell lines. One of three independent experiments with similar results is shown. (b) Effect of depsipeptide on histone deacetylation in B16/F10 cells. B16/F10 cells ( $2 \times 10^6$ ) were exposed to depsipeptide at the indicated concentration for 16 hours. Cells were lysed and analyzed for anti-acetyl-histone H3 (Lys 9), anti-acetyl-histone H3 (Lys 18) and anti-histone H3 by western blotting. (c) Expression of MHC class I (H2-D<sup>b</sup>) and Fas (CD95) in B16/F10 cells following exposure to depsipeptide. B16/F10 cells were exposed to depsipeptide at the indicated concentration for 16 hours and stained with PE-conjugated anti-H2D<sup>b</sup> or Fas mAb. The control was treated with PBS. One of 2–3 independent experiments with similar results is shown.

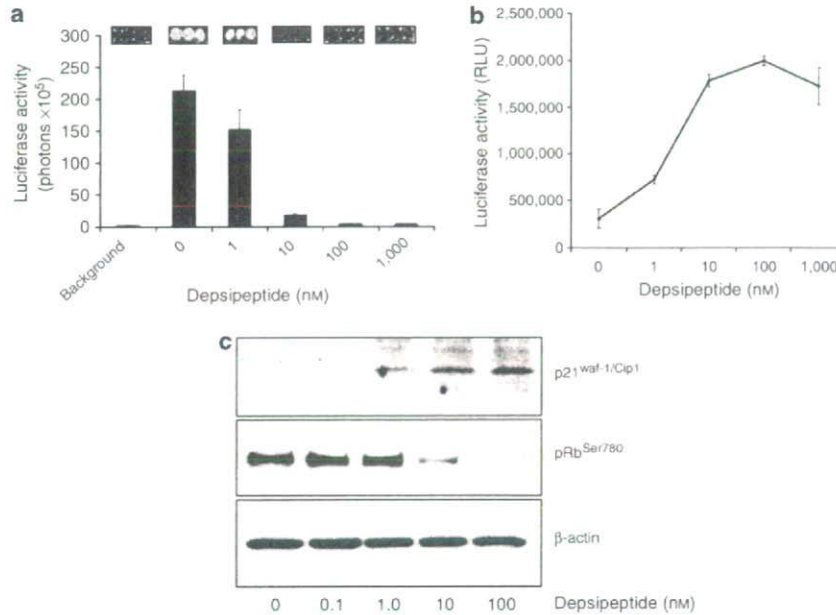


**Figure 2. Depsipeptide activates caspase-3/7 and accompanies cell cycle arrest in B16/F10 cells.** (a) Luc-B16/F10 cells ( $1 \times 10^5$ ) were plated onto 48-well plates at the indicated number and exposed to depsipeptide at the indicated concentration for 16 hours. Luciferase activity (photon counts) was then evaluated in the presence of *D*-luciferin. (b) Caspase-3/7 activity was quantified for 16 hours following treatment at the indicated concentration of depsipeptide in B16/F10 cells ( $2 \times 10^4$ ). The Caspase-Glo 3/7 Assay system (Promega) was used according to the manufacturer's instructions. The background luminescence associated with the cell culture and assay reagent (blank reaction) was subtracted from experimental values. (c) Western blot analysis of p21<sup>Waf1/Cip1</sup> and phospho-RB (Ser780) 16 hours following treatment at the indicated concentration of depsipeptide.  $\beta$ -actin was used as an internal control. One of two independent experiments with similar results is shown.

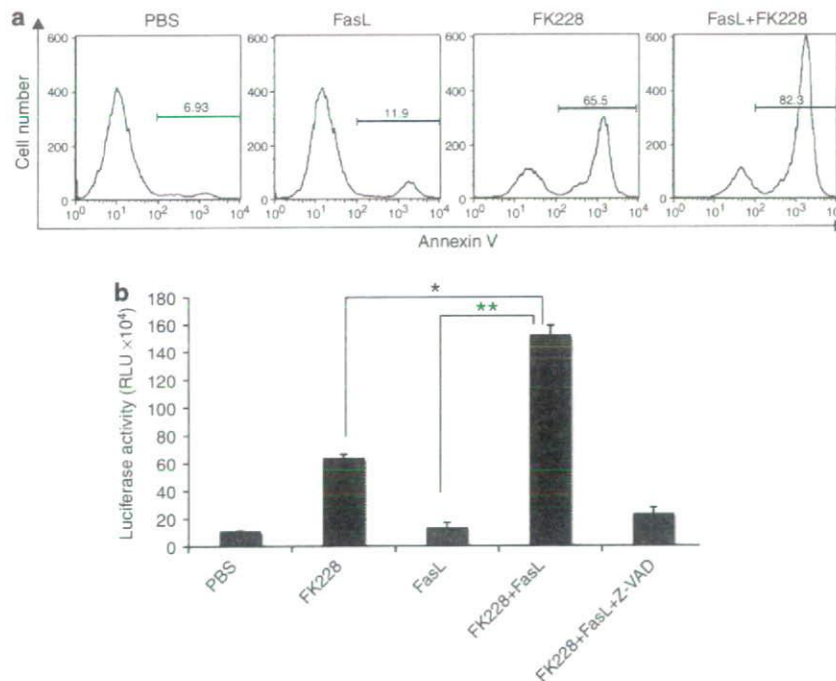


**Figure 3. A sublethal dose of depsipeptide with Fas engagement synergistically promotes apoptotic cell death in B16/F10 cells *in vitro*.** (a) B16/F10 cells ( $1 \times 10^5$ ) were treated with depsipeptide (5 nm) and recombinant FLAG-tagged FasL ( $10 \text{ ng ml}^{-1}$ ) and multimerized with anti-FLAG M2 antibodies ( $1 \text{ mg ml}^{-1}$ ) for 16 hours. Cells were then collected and stained with annexin-V-FITC. One of two independent experiments with similar results is shown. (b) Caspase-3/7 activity after exposure to depsipeptide with Fas engagement. The Caspase-Glo 3/7 Assay system (Promega) was used as described above. \* $P < 0.05$ ; \*\* $P < 0.001$  (Student's *t*-test).



et al., 2006). As photon emission from luciferase-expressing luc-B16/F10 cells was highly correlated with viable cell number (Sato et al., 2006), we examined a sublethal dose of depsipeptide on murine B16/F10 melanoma cells (Figure 2a). Results revealed that depsipeptide decreased tumor-derived photons in a dose-dependent manner. Furthermore, caspase-3/7 activity in unmanipulated B16/F10 cells also increased linearly after a 24 hour exposure to 1–10 nM depsipeptide (Figure 2b), with the median dose of depsipeptide (ED<sub>50</sub>) being 5.34 nM. The increase in caspase-3/7 activity was accompanied by a dose-dependent increase in the expression of the cell cycle regulator p21<sup>Waf/Cip1</sup>, and the Rb protein was dephosphorylated at the critical residue Ser<sup>780</sup> for the cell cycle (Figure 2c). Thus, a sublethal dose of depsipeptide could moderately induce apoptosis and cell cycle arrest in murine B16/F10 melanoma cells.

**Depsipeptide with Fas death receptor engagement synergistically promotes apoptosis in B16/F10 melanoma cells**

In mechanisms associated with lymphocyte-mediated tumor killing, the Fas and Fas ligand (FasL) system is a well-known major pathway in mice (Kagi et al., 1994; Caldwell et al., 2003; Lee et al., 2006). We therefore examined whether a sublethal dose of depsipeptide (ED<sub>50</sub>: 5 nM) promoted FasL-triggered apoptosis. B16/F10 cells were exposed to depsipeptide in the presence or absence of multimerized FasL, which was measured by annexin-V staining (Figure 3a). In the presence of depsipeptide, B16/F10 cells readily induced apoptotic cell death after Fas–FasL crosslinking, whereas B16/F10 cells were resistant to apoptosis with Fas crosslinking alone. Caspase-3/7 activity was also synergistically enhanced in the presence of depsipeptide and FasL (Figure 3b). Pan-caspase inhibition in tumor cells treated with Z-VAD-fmk almost totally cancelled the enhanced cytotoxic effect.

We next investigated whether a sublethal dose of depsipeptide promoted cytotoxicity induced by melanoma antigen-specific cytotoxic T lymphocytes (CTLs). To generate B16/F10-specific CTLs, C57BL/6 mice were immunized twice by subcutaneous (s.c.) injection of irradiated IL-12/IL-18-transduced B16/F10 cells (Sato et al., 2006). Spleen cells from immunized mice showed enhanced production of IFN- $\gamma$  (Figure 4a) and moderate killing activity with respect to B16/F10 cells (data not shown). Strikingly, the spleen cells demonstrated efficient killing of luc-B16/F10 cells in the presence of depsipeptide (Figure 4b). Furthermore, we investigated whether depsipeptide-exposed luc-B16/F10 cells could be killed by CD8<sup>+</sup> T cells from a transgenic mouse (Pmel-1), which expressed V $\alpha$ 2V $\beta$ 13 TCR from H-2D<sup>b</sup>-restricted murine gp100-specific clone no. 9 T cells (Overwijk et al., 2003). As shown in Figure 5a, Pmel-1 T cells were also capable of efficiently killing depsipeptide-exposed luc-B16/F10 cells. Depsipeptide at 5 nM moderately enhanced the surface expression of FasL in antigen-activated Pmel-1 T cells (Figure 5b). Furthermore, to examine whether pmel-1 CTL killing of luc-B16/F10 was primarily mediated by Fas–FasL-dependent pathway, we assessed the effect of anti-FasL neutralizing antibodies on the luc-B16/F10 killing. Anti-FasL mAb (20  $\mu$ g ml<sup>-1</sup>) inhibited Pmel-mediated killing of

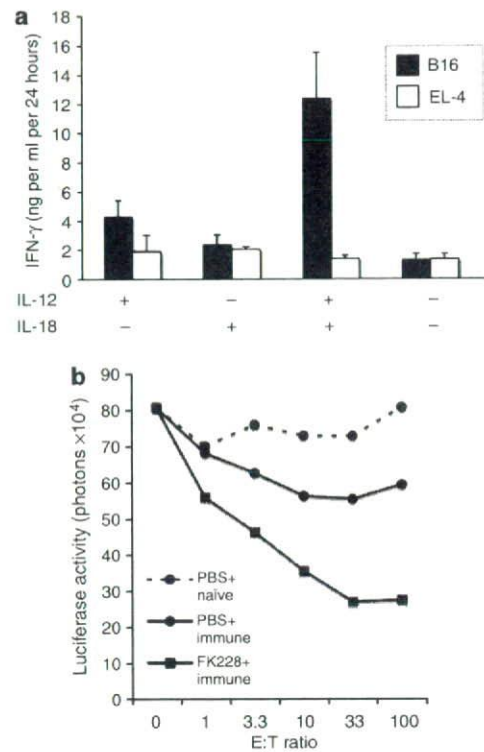


**Figure 4. Melanoma-specific CTLs with depsipeptide can synergistically kill B16/F10 cells *in vitro*.** (a) IFN- $\gamma$  levels from splenocytes were assayed by ELISA. Splenocytes ( $2 \times 10^5$ ) were isolated after the second immunization using irradiated IL-12/IL-18 cDNA-transduced B16/F10 cells and were co-cultured for 24 hours with  $1 \times 10^5$  target cells (irradiated with 80 Gy). The IFN- $\gamma$  concentration of the supernatants was measured using a mouse IFN- $\gamma$  immunoassay kit (R&D Systems, Minneapolis, MN) according to the manufacturer's instructions. EL-4 thymoma cells were used for control H-2<sup>b</sup> tumor cells for a B16-specific IFN- $\gamma$  increase. Error bar, SD ( $n=3$ ). A representative result of three independent experiments with similar results is shown. (b) Cytotoxic assay against depsipeptide-exposed luc-B16/F10 cells. C57BL/6 mice were immunized by s.c. injection of irradiated IL-12/IL-18 cDNA-transduced B16/F10 cells. Spleen cells were isolated and used as effectors at the indicated effector-to-target (E:T) ratios. Photons represent cell viability from luc-B16/F10 cells 10 hours following incubation with effector lymphocytes. Data are shown as the average of triplicate assays.

depsipeptide-treated luc-B16/F10 cells at lower effector-to-target ratios (Figure 5c). This anti-FasL mAb could not sufficiently block the Pmel-mediated killing even at a high concentration (50  $\mu$ g ml<sup>-1</sup>, Figure 5d). Thus, in regard to the mechanism underlying the synergistic effect of depsipeptide and CTL cells, the CTL-mediated killing of B16 cells was not completely dependent on Fas–FasL interactions.

**Depsipeptide increases perforin in activated CD8<sup>+</sup> T lymphocytes**

We further addressed the effects of depsipeptide on activated CD8<sup>+</sup> T cells *in vitro*. The trypan blue exclusion test showed that depsipeptide at 5 nM had little effect on viability of antigen-activated Pmel-1 CTLs within 24 hours (data not shown). An alternative hypothesis is that depsipeptide may enhance immune effector cell function to produce the

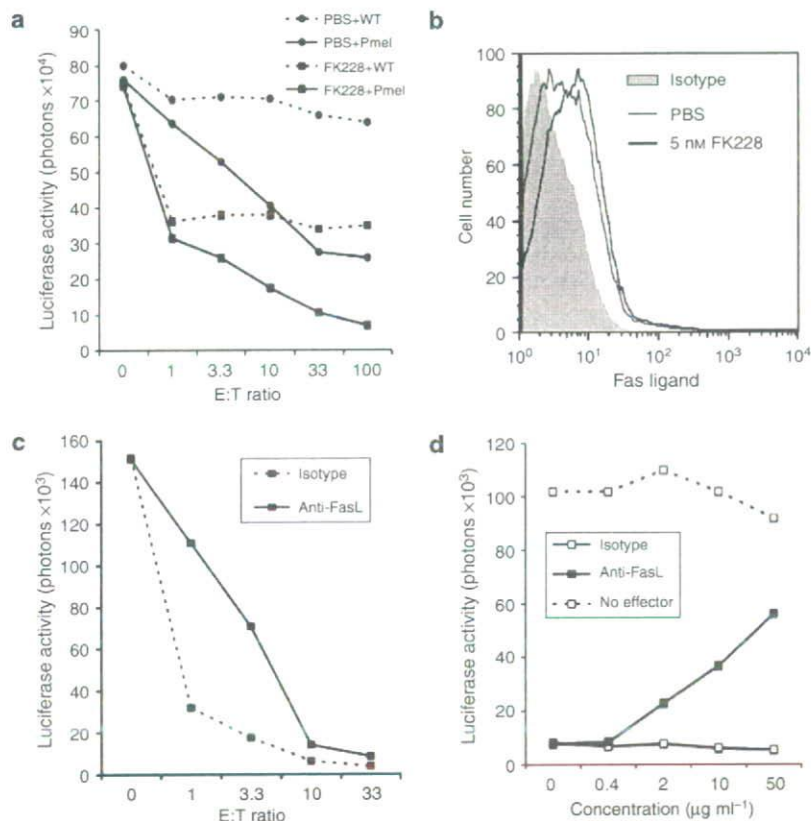


**Figure 5.** Gp100-specific CTLs with depsipeptide can synergistically kill B16/F10 cells *in vitro*. (a) Killing of depsipeptide-exposed luc-B16/F10 cells by gp100-specific CD8<sup>+</sup> T cells from a transgenic mouse (Pmel-1). Pmel-1 cells were used as effectors at the indicated effector-to-target (E:T) ratios. One of three independent experiments with similar results is shown. (b) Expression of FasL (CD178) in Pmel-1 T cells following exposure to depsipeptide. Antigen-stimulated Pmel-1 T cells were exposed to depsipeptide at 5 nM for 16 hours and stained with PE-conjugated anti-FasL mAb. (c) Effect of neutralizing anti-FasL mAb on Pmel-1 CTL-mediated B16/F10 killing. Depsipeptide (5 nM)-exposed luc-B16/F10 cells were co-incubated with Pmel-1 CTLs for 16 hours in the presence of anti-FasL mAb (20 μg ml<sup>-1</sup>) or isotype-matched control Ab (20 μg ml<sup>-1</sup>). (d) Depsipeptide (5 nM)-exposed luc-B16/F10 cells were incubated with Pmel-1 CTLs at a 10:1 (E:T) ratio for 16 hours with various concentrations of anti-FasL mAb. One of two independent experiments with similar results is shown.

antitumor response. Pmel-1 T cells were exposed to depsipeptide in the presence or absence of antigen stimulation, and expression of perforin was analyzed using flow cytometry (Figure 6a). Although perforin expression levels did not alter in unstimulated Pmel-1 T cells following exposure to 5 nM depsipeptide for 24 hours, cells that express perforin increased in antigen-stimulated Pmel-1 T cells. To address whether perforin mRNA expression in Pmel-1 T cells could be altered by exposure to depsipeptide, RT-PCR analysis was performed (Figure 6b). The results demonstrated that levels of perforin mRNA did not alter following exposure to multiple concentrations of depsipeptide. These results, therefore, suggest that perforin expression by exposure to depsipeptide is regulated at post-transcriptional levels. An increase of perforin was also observed in healthy human peripheral CD8<sup>+</sup> T cells stimulated with phytohemagglutinin-P (PHA-P) for 24 hours (Figure 6c) and an accumulation of perforin was observed in a small number of these T cells (Figure S2). These results suggest that depsipeptide potentially increases the number of cells that express perforin in murine-activated

CD8<sup>+</sup> T cells and that it enhances intracellular perforin accumulation in human T cells. These results may support the notion of an antitumor response in the host.

#### Inhibition of tumor growth of B16/F10 by a combination of depsipeptide with immune cell adoptive transfer therapy

To examine whether a sublethal dose of depsipeptide sensitizes B16/F10 cells *in vivo* for adoptive immunotherapy, growth retardation of established B16/F10 s.c. tumor in C57BL/6 mice (see Materials and Methods) was monitored after intraperitoneal injection of depsipeptide and subsequent adoptive transfer of Pmel-1 CTLs (Figure 7a). Depsipeptide intraperitoneal administration was performed for 3 days at the indicated doses. Established B16/F10 s.c. tumor growth was retarded with 2 mg kg<sup>-1</sup> of depsipeptide at 7 days post-Pmel-1 CTL transfer. The acetylation level of histone H3 (lysine 18) also increased following depsipeptide treatment at target tumor sites (Figure 7b). Notably, this modulation was preferentially observed in the margin and perivascular area of the formed tumor (Figure S3a). A moderate induction



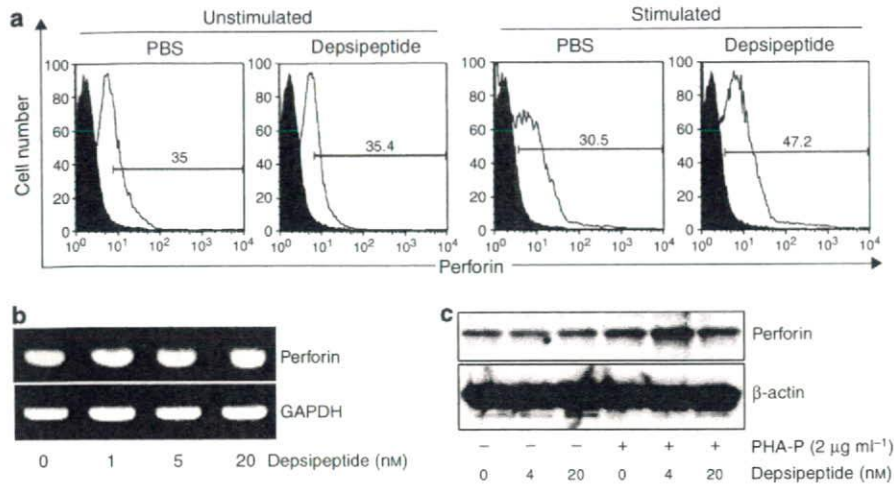


**Figure 6.** Effect of depsipeptide on perforin expression in effector T cells. (a) Increase of perforin-expressing antigen-stimulated pmel-1 T cells by exposure to depsipeptide (5 nM). Primary or antigen-stimulated Pmel-1 T cells (Thy1.1<sup>+</sup>) with or without depsipeptide (5 nM) for 16 hours were stained by FITC-conjugated anti-mouse perforin mAb after treatment with a Fixation & Permeabilization Kit (eBioscience). Shaded area represents isotype-matched control staining. (b) Antigen-stimulated Pmel-1 T cells were treated with depsipeptide at various concentrations for 16 hours, and then perforin mRNA was analyzed by RT-PCR (glyceraldehyde-3-phosphate dehydrogenase (GAPDH), an internal control). (c) Human CD8<sup>+</sup> T cells were purified from peripheral blood mononuclear cells of healthy volunteers by magnetic bead selection and stimulated with or without PHA-P (2 μg ml<sup>-1</sup>) *in vitro* for 24 hours. Cells were then lysed and probed for perforin and actin (as an internal control) by western blotting.

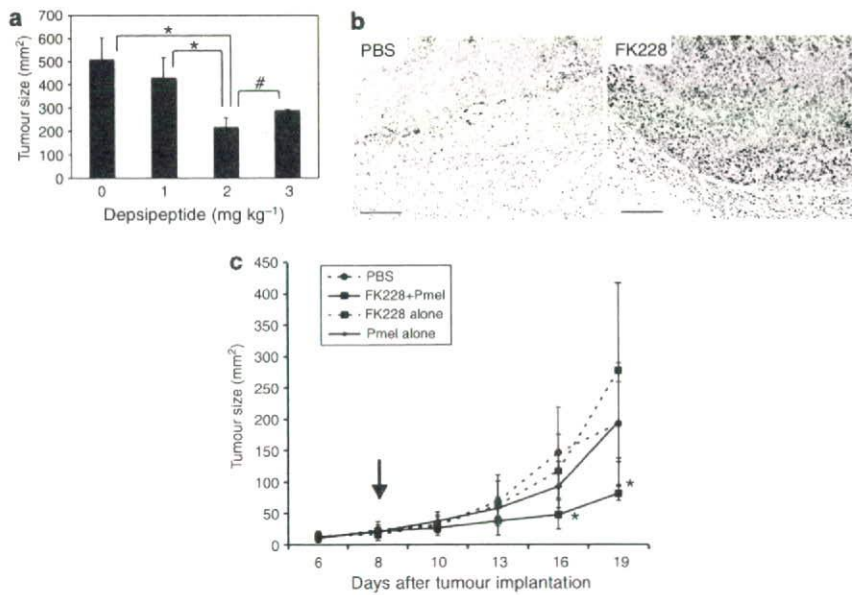


**Figure 7.** A limited dose of depsipeptide enhances CTL-mediated Luc-B16/F10 cell killing *in vivo*. (a) Effect of depsipeptide on B16/F10 tumor growth *in vivo*. B16/F10 cells ( $1 \times 10^6$ ) were inoculated subcutaneously into the abdominal skin of mice (day 0). A visible tumor in each mouse was established at day 7 after tumor implantation (average size:  $122 \pm 20 \text{ mm}^2$ ), and mice were randomized and divided into four groups before treatment. Depsipeptide was administered intraperitoneally into mice from days 7–9 (only for 3 days) at the indicated dose, and activated Pmel-T cells ( $4 \times 10^6$ ) were subsequently injected intravenously into the tail vein of mice. Tumor growth was measured at day 21 after tumor implantation. The error bars represent the mean  $\pm$  SD ( $n = 4$ ). \* $P < 0.05$ ; # $P > 0.3$  (Mann–Whitney *U*-test). (b) Effect of depsipeptide on histone deacetylation in a subcutaneous tumor of B16/F10 cells. Established B16/F10 skin tumors 1 day after the final depsipeptide administration ( $2 \text{ mg kg}^{-1}$ ) were probed for acetyl-histone H3 (Lys 18) by immunohistochemistry (Bar =  $100 \mu\text{m}$ ). (c) Depsipeptide enhances CTL-mediated B16/F10 tumor killing *in vivo*. B16/F10 cells ( $5 \times 10^3$ ) were inoculated subcutaneously into the abdominal skin of mice (day 0). A visible tumor in each mouse was established at day 5 after tumor implantation. Depsipeptide ( $2 \text{ mg kg}^{-1}$ ) was administered intraperitoneally into mice from days 6–8 (for 3 days), and Pmel-1 CTLs ( $4 \times 10^6$ ) were subsequently injected intravenously into the tail vein of mice (indicated by the arrow). Tumor growth was monitored every 2–3 days after tumor implantation. The error bars represent the mean  $\pm$  SD ( $n = 5–6$ ). \* $P < 0.05$  (Kruskal–Wallis test; at days 16 and 19 after tumor implantation). One of three independent experiments with similar results is shown.